target site, that is, to examine that there are no highly homologous sequences in other genes. Under what conditions should one check the specificity? If very stringent conditions are applied, for example, more than three base mismatches are needed to determine the discrimination between the correct and homologous targets, significant portions of favorable target sites that were predicted as highly active sites could be eliminated by the BLAST search program. On the other hand, if less stringent conditions are applied, for example, only one base mismatch is allowed for the discrimination, the designed siRNA might have the potential to disrupt not only the correct target but also other homologous genes as well, although the cleavage efficiency is reduced for the latter. Under these circumstances, we have decided to use the relatively low stringent condition for examining target site specificity, because multiple positive candidates can be further analyzed by creating new siRNAs targeted at different sites within the candidate gene.

Alternative splicing and highly homologous gene families are also major problems for target site selection. Recent genome-wide analysis of transcripts reveals that many genes have alternative splicing forms. For example, in case where one tries to disrupt a specific alternative variant, an siRNA expression vector targeted against the specific variant can be created, without damaging other alternative variants originating from the same pre-spliced form. However, for the generation of the first draft library, in the targeting of genes which have multiple alternative splicing forms, the common sequence of all alternative transcripts (similarly, the common sequence for the homologous gene family) can be aimed as a target site. This is more economical for the creation of the first library and additional siRNAs can easily be made once the targeted gene is identified as being an attractive candidate.

3.7. Improved method for library construction

In constructing an siRNA expression library against all genes in the genome, one would become focused on practical problems, such as how to construct the library efficiently, rapidly, and at a reduced price.

We have established a large-scale method for constructing a library, as shown in Fig. 4. Specifically, 96 sets of oligonucleotides that include hairpin sequences corresponding to 96 target sequences were synthesized and annealed separately. Then the annealed oligonucleotides were mixed, and were ligated into *Bsp*MI site of the U6-driven siRNA expression vector. After transformation into *E. coli*, 384 clones were picked up and were sequenced to identify each clone. In our data, about 88.5% of the clones were recovered in a single procedure. The unrecovered clones were followed by the next round of the construction. This bulk procedure allowed the production of an siRNA expression vector dramatically cheaper and faster than the traditional procedure in which each clone is made separately. Using this procedure, we can practically make 3000–5000 siRNA expression vectors per month (Taira and Miyagishi, 2001).

3.8. Advantages and disadvantages of siRNA expression library compared to siRNA oligonucleotide library

For the plasmid-based siRNA expression library and the alternative oligonucleotide-based siRNA library, there are advantages and disadvantages.

Transfection efficiency of siRNA into cells using lipofection depends on cell types and the RNAi effect only seems to be sustained for a period of time. The advantage of the plasmid-based siRNA is the capability of removing those cells that were not transfected with the plasmids by selecting the transfected cells with antibiotic resistant genes. Moreover, the RNAi effect lasts for much longer periods when plasmid-based siRNAs are used. Additionally, virus vectors enable us to deliver siRNA expression cassettes into cells with higher transfection efficiency, and in the case of lentivirus and retrovirus, it is easy to make stable knockdown cells by the integration of the virus vector into the genome. If one wants to use siRNA expression vectors as a bulk library, these virus vectors, which can generate stable knockdown cells, would be most suitable for the bulk library screen.

The advantage of oligonucleotide-based siRNA is that, in some favorable cells, transfection efficiency is greater than 90%, and thus higher than that of the plasmid. However, for the library, once plasmid-based siRNAs are generated, they can be amplified unlimitedly, especially with our construct (Fig. 2B) which does not undergo unwanted mutation (unlike conventional ones) during amplification in *E. coli* cells, resulting in a more economical construction of a library set.

4. Conclusions

During the present work, we have developed a genetically stable and highly active siRNA expression vector, and have established a system for constructing high-quality and genome-wide scale siRNA expression libraries very efficiently. Recently, we have started to screen functional genes by using the constructed siRNA-expression library. Fig. 5 shows an example of screening of functional genes in the apoptosis pathway. Positive controls (siRNA-expression vectors targeted against PKR) could block dsRNA-induced apoptosis (Fig. 5A), and in the experiments using siRNA expression vectors targeted against unknown genes (Fig. 5B; C1–C11), one positive clone could be identified fron 11 candidates (Fig. 5B; C7). Within the next few years, several groups, including our own would expect to identify a number of genes through the use of various siRNA libraries. In the past, we were able to identify miRNA sequences by our ribozyme library (Kuwabara et al., 2004). Since miRNA plays an important role in development, and possibly in other

biological phenomena of mammalian cells (Kawasaki et al., 2004), the siRNA library should also cover miRNAs and undefined noncoding RNAs as targets. Scientists are making the first great step in functional genome analysis, and human beings will soon enjoy deeper knowledge of the unraveled life of cells.

References

Beger, C., Pierce, L.N., Kruger, M., Marcusson, E.G., Robbins, J.M., Welcsh, P., Welch, P.J., Welte, K., King, M.C., Barber, J.R., Wong-Staal, F., 2001. Identification of Id4 as a regulator of BRCA1 expression by using a ribozyme-library-based inverse genomics approach. Proc. Natl. Acad. Sci. U.S.A. 98, 130–135.

Brummelkamp, T.R., Bernards, R., Agami, R., 2002. A system for stable expression of short interfering RNAs in mammalian cells. Science 296, 550–553.

Caplen, N.J., Parrish, S., Imani, F., Fire, A., Morgan, R.A., 2001. Specific inhibition of gene expression by small double-stranded RNAs in invertebrate and vertebrate systems. Proc. Natl. Acad. Sci. U.S.A. 98, 9742–9747.

Elbashir, S.M., Harborth, J., Lendeckel, W., Yalcin, A., Weber, K., Tuschl, T., 2001. Duplexes of 21-nucleotide RNAs mediate RNA interference in cultured mammalian cells. Nature 411, 494–498.

Fire, A., Xu, S., Montgomery, M.K., Kostas, S.A., Driver, S.E., Mello, C.C., 1998. Potent and specific genetic interference by double-stranded RNA in *Caenorhabditis elegans*. Nature 391, 806–811.

Fraser, A.G., Kamath, R.S., Zipperlen, P., Martinez-Campos, M., Sohrmann, M., Ahringer, J., 2000. Functional genomic analysis of *C. elegans* chromosome I by systematic RNA interference. Nature 408, 325–330.

Gonczy, P., Echeverri, C., Oegema, K., Coulson, A., Jones, S.J., Copley, R.R., Duperon, J., Oegema, J., Brehm, M., Cassin, E., Hannak, E., Kirkham, M., Pichler, S., Flohrs, K., Goessen, A., Leidel, S., Alleaume, A.M., Martin, C., Ozlu, N., Bork, P., Hyman, A.A., 2000. Functional genomic analysis of cell division in *C. elegans* using RNAi of genes on chromosome III. Nature 408, 331–336.

Kawasaki, H., Taira, K., 2002. Identification of genes by hybrid ribozymes that couple cleavage activity with the unwinding activity of an endogenous RNA helicase. EMBO Rep. 3, 443–450.

Kawasaki, H., Taira, K., 2003. Short hairpin type of dsRNAs that are controlled by $tRNA^{Val}$ promoter significantly induce RNAi-mediated gene silencing in the cytoplasm of human cells. Nucleic Acids Res. 31, 700–707.

Kawasaki, H., Onuki, R., Suyama, E., Taira, K., 2002. Identification of genes that function in the TNF-alpha-mediated apoptotic pathway using randomized hybrid ribozyme libraries. Nat. Biotechnol. 20, 376–380.

Kawasaki, H., Wadhwa, R., Taira, K., 2004. World of small RNAs: from ribozymes to siRNA and miRNA. Differentiation, in press.

Ketting, R.F., Fischer, S.E., Bernstein, E., Sijen, T., Hannon, G.J., Plasterk, R.H., 2001. Dicer functions in RNA interference and in synthesis of small RNA involved in developmental timing in *Caenorhabditis elegans*. Genes Dev. 15, 2654–2659.

Kruger, M., Beger, C., Li, Q.X., Welch, P.J., Tritz, R., Leavitt, M., Barber, J.R., Wong-Staal, F., 2000. Identification of eIF2Bgamma and eIF2gamma as cofactors of hepatitis C virus internal ribosome entry site-mediated translation using a functional genomics approach. Proc. Natl. Acad. Sci. U.S.A. 97, 8566–8571.

Kuwabara, T., Hsieh, J., Nakashima, K., Taira, K., Gage, F.H., 2004. Small Modulatory dsRNA specifies the Fate of Adult Neural Stem Cells. Cell, in press.

Lee, N.S., Dohjima, T., Bauer, G., Li, H., Li, M.J., Ehsani, A., Salvaterra, P., Rossi, J., 2002. Expression of small interfering RNAs targeted against HIV-1 rev transcripts in human cells. Nat. Biotechnol. 20, 500–505.

Li, Q.X., Robbins, J.M., Welch, P.J., Wong-Staal, F., Barber, J.R., 2000. A novel functional genomics approach identifies mTERT as a suppressor of fibroblast transformation. Nucleic Acids Res. 28, 2605–2612.

Lindberg, W., Persson, J.A., Wold, S., 1983. Partial least-squares method for spectrofluorimetric analysis of mixtures of humic acid and lignin sulfonate. Anal. Chem. 55, 643–648.

McManus, M.T., Sharp, P.A., 2002. Gene silencing in mammals by small interfering RNAs. Nat. Rev. Genet. 3, 737–747.

Miyagishi, M., Taira, K., 2002. U6 promoter-driven siRNAs with four uridine 3′ overhangs efficiently suppress targeted gene expression in mammalian cells. Nat. Biotechnol. 20, 497–500.

Miyagishi, M., Taira, K., 2003. Expression of siRNA from a pol III promoter in mammalian cells. In: Appasani, K. (Ed.), Perspectives in Gene Expression, The Eaton Publishers, Westboro, MA. pp. 361–376.

Miyagishi, M., Fujii, R., Hatta, M., Yoshida, E., Araya, N., Nagafuchi, A., Ishihara, S., Nakajima, T., Fukamizu, A., 2000. Regulation of Lef-mediated transcription and p53-dependent pathway by associating β-catenin with CBP/p300. J. Biol. Chem. 275, 35170–35175.

Miyagishi, M., Suminoto, H., Miyoshi, H., Kawakami, Y., Taira, K., 2004. Optimization of an siRNA-expression system with a mutated hairpin and its significant suppressive effects upon HIV vector-mediated transfer into mammalian cells. J. Gene Med., in press.

Onuki, R., Nagasaki, A., Kawasaki, H., Baba, T., Uyeda, T.Q., Taira, K., 2002. Confirmation by FRET in individual living cells of the absence of significant amyloid beta-mediated caspase 8 activation. Proc. Natl. Acad. Sci. U.S.A. 99, 14716–14721.

Paddison, P.J., Caudy, A.A., Bernstein, E., Hannon, G.J., Conklin, D.S., 2002. Short hairpin RNAs (shRNAs) induce sequence-specific silencing in mammalian cells. Genes Dev. 16, 948–958.

Paul, C.P., Good, P.D., Winer, I., Engelke, D.R., 2002. Effective expression of small interfering RNA in human cells. Nat. Biotechnol. 20, 505–508.

Rhoades, K., Wong-Staal, F., 2003. Inverse Genomics as a powerful tool to identify novel targets for the treatment of neurodegenerative diseases. Mech. Ageing Dev. 124, 125–132.

Sui, G., Soohoo, C., Affarel, B., Gay, F., Shi, Y., Forrester, W.C., Shi, Y., 2002. A DNA vector-based RNAi technology to suppress gene expression in mammalian cells. Proc. Natl. Acad. Sci. U.S.A. 99, 5515–5520.

Suyama, E., Kawasaki, H., Kasaoka, T., Taira, K., 2003a. Identification of genes responsible for cell migration by a library of randomized ribozymes. Cancer Res. 63, 119–124.

Suyama, E., Kawasaki, H., Nakajima, M., Taira, K., 2003b. Identification of genes involved in cell invasion by using a library of randomized hybrid ribozymes. Proc. Natl. Acad. Sci. U.S.A. 100, 5616–5621.

Taira, K., Miyagishi, M., 2001. siRNA Expression System and Method for Producing Functional Gene Knock-down Cell Using the System. Japanese Patent Application, Heiser–13–363385 (PCT/JP02/12447).

Tuschl, T., 2002. Expanding small RNA interference. Nat. Biotechnol. 20, 446–448.

Warashina, M., Kuwabara, T., Kato, Y., Sano, M., Taira, K., 2001. RNA-protein hybrid ribozymes that efficiently cleave any mRNA independently of the structure of the target RNA. Proc. Natl. Acad. Sci. U.S.A. 98, 5572–5577.

Welch, P.J., Marcusson, E.G., Li, Q.X., Beger, C., Kruger, M., Zhou, C., Leavitt, M., Wong-Staal, F., Barber, J.R., 2000. Identification and validation of a gene involved in anchorage-independent cell growth control using a library of randomized hairpin ribozymes. Genomics 66, 74–83.

Yu, J.Y., DeRuiter, S.L., Turner, D.L., 2002. RNA interference by expression of short-interfering RNAs and hairpin RNAs in mammalian cells. Proc. Natl. Acad. Sci. U.S.A. 99, 6047–6052.

Zamore, P.D., 2001. RNA interference: listening to the sound of silence. Nat. Struct. Biol. 8, 746–750.

Oncogene (2004) 23, 6031–6039

www.nature.com/onc

Inhibition of growth and invasive ability of melanoma by inactivation of mutated BRAF with lentivirus-mediated RNA interference

Hidetoshi Sumimoto[1], Makoto Miyagishi[2], Hiroyuki Miyoshi[3], Shizuko Yamagata[1], Ayako Shimizu[1], Kazunari Taira[2] and Yutaka Kawakami*[,1]

[1]*Division of Cellular Signaling, Institute for Advanced Medical Research, Keio University School of Medicine, 35 Shinanomachi, Shinjuku-ku, Tokyo 160-8582, Japan;* [2]*Department of Chemistry and Biotechnology, School of Engineering, The University of Tokyo, Hongo, Tokyo 113-8656, Japan;* [3]*Subteam for Manipulation of Cell Fate, BioResource Center, RIKEN Tsukuba Institute, 3-1-1 Koyadai, Tsukuba 305-0074, Japan*

Oncogenic mutations of molecules involved in the mitogen-activated protein kinase (MAPK) pathways provide signals mediating both tumor growth and invasion in various cancers including melanomas. BRAF somatic mutations, found in 66% of melanomas, have NIH3T3 transforming ability with the elevated kinase activity *in vitro*. We attempted to mediate RNA interference (RNAi) with HIV lentiviral vectors specific for either wild type or the most frequently mutated form of BRAF (V599E) in 10 melanoma cell lines, and found that RNAi inhibited the growth of most melanoma cell lines *in vitro* as well as *in vivo*, which was accompanied by decrease of both BRAF protein and ERK phosphorylation. Interestingly, the mutated BRAF (V599E)-specific siRNA inhibited the growth and MAPK activity of only melanoma cell lines with this mutation. Furthermore, BRAF RNAi inhibited matrigel invasion of melanoma cells accompanied with a decrease of matrix metalloproteinase activity and β_1 integrin expression. These results clarify that the mutated BRAF (V599E) is essentially involved in malignant phenotype of melanoma cells through the MAPK activation and is an attractive molecular target for melanoma treatment. The lentivirus-mediated RNAi specific for oncogenic mutations may be a powerful technique for gene therapy of cancer.
Oncogene (2004) **23**, 6031–6039. doi:10.1038/sj.onc.1207812
Published online 21 June 2004

Keywords: gene therapy; melanoma; lentiviral vector; BRAF; RNAi; MAPK

Introduction

RNA interference (RNAi) is an evolutionarily conserved process whereby double-stranded RNA (dsRNA) induces a sequence-specific degradation of homologous mRNA, leading to post-transcriptional gene silencing (Hannon, 2002). This involves cleavage of dsRNA into short (21–23 nt) small interfering RNAs (siRNAs) with characteristic 2 nt 3′-overhanging ends, which is mediated by Dicer (Bernstein *et al.*, 2001). However, in mammalian cells, dsRNA larger than 30 base pairs can trigger an interferon response that globally represses gene expression. This nonspecific gene silencing effect could be avoided by introducing synthetic siRNAs of 21 nt lengths (Elbashir *et al.*, 2001) or siRNA expression vectors (Tuschl, 2002) into mammalian cells.

The Ras/Raf/MEK/ERK pathway is one of the major signal transduction pathway involved in cellular growth (Cobb, 1999). Many melanomas are known to have activating mutations of either N-Ras or BRAF, suggesting that the downstream effector ERK may play a major role in the malignant phenotype of melanoma (Smalley, 2003). BRAF missense mutations were found in 66% of melanomas and all of the mutations located within the kinase domain, particularly with a single substitution (T→A) of glutamic acid for valine (V599E) in 80% of theses mutations (Davies *et al.*, 2002). These mutations were associated with a 10–12-fold increase of the kinase activity and a 70–138-fold increase of transformation ability in NIH3T3 cells (Davies *et al.*, 2002). These results indicated that these BRAF mutations were involved in oncogenic transformation of melanoma and may be good targets for treatment.

However, the effects of the mutated BRAF observed in the transient transfection into COS or NIH3T3 cells might have overestimated the activity of mutated BRAF because of much higher expression than actual *in vivo* expression. Thus, it is important to evaluate the role of the mutated BRAF on the activation of mitogen-activated protein kinase (MAPK) pathway and cellular growth at a more pathophysiological level particularly when considering BRAF as a therapeutic target, which has not been extensively investigated. Therefore, we have attempted to evaluate effects of the mutated and wild-type BRAF on proliferation and invasive ability of melanoma cells by suppressing the BRAF expression with RNAi using lentiviral vectors in mutation-specific and nonspecific ways. Since the gene silencing effect by RNAi is highly sequence-specific, allowing discrimination of only a single base substitution (Brummelkamp *et al.*, 2002a, b; Kawasaki and Taira, 2003), BRAF V599E missense mutation-specific RNAi was attempted.

*Correspondence: Y Kawakami; E-mail: yutakawa@sc.itc.keio.ac.jp
Received 3 December 2003; revised 7 April 2004; accepted 15 April 2004; published online 21 June 2004

Although several siRNA expression systems using plasmid vectors (Lee *et al*., 2002; Miyagishi and Taira, 2002; Paddison *et al*., 2002; Paul *et al*., 2002; Sui *et al*., 2002; Yu *et al*., 2002; Kawasaki and Taira, 2003) or viral vectors (Abbas-Terki *et al*., 2002; Barton and Medzhitov, 2002; Brummelkamp *et al*., 2002b; Devroe and Silver, 2002; Xia *et al*., 2002; Qin *et al*., 2003; Rubinson *et al*., 2003; Tiscornia *et al*., 2003) containing RNA Pol III promoters have been reported, we used a lentiviral vector for siRNA expression because of its high transduction ability on various types of cells and stable gene transduction for long-term RNAi effects. We found that *in vitro* and *in vivo* growth and *in vitro* invasive ability of melanoma cells were inhibited by infecting lentivirus vectors expressing siRNAs for BRAF, indicating that BRAF is an excellent molecular target for the treatment of melanoma, including gene therapy.

Results

siRNA-expressing HIV vectors for BRAF

Three siRNA target sites, #1′ including the V599E mutation, and #10 and #7′ without the mutation, were selected within the coding region of the BRAF mRNA. We constructed three siRNA-expressing HIV vectors specific for these three target sites. The HIV vector contains an siRNA expression unit (human U6 promoter and two *Bsp*MI cloning sites) between central termination sequence (CTS) and a green fluorescence protein (GFP) expression unit (Figure 1a) (Miyagishi *et al*., in press). The synthetic oligonucleotides (the target sense – linker – the target antisense – stop sequence (TTTTT)) were subcloned into the two *Bsp*MI sites. The siRNAs were produced by human U6 promoters as a fold-back stem–loop structure. Transduction efficiency was monitored by evaluating GFP expression.

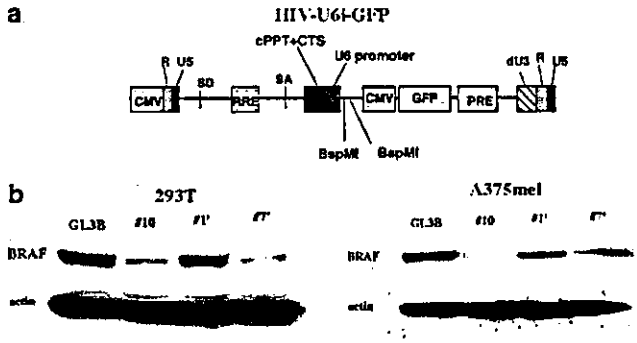

Figure 1 HIV vectors expressing siRNAs for BRAF. (a) The genomic structure of an HIV vector containing an siRNA expression cassette. The cassette consists of one U6 promoter and two *Bsp*MI cloning sites, into which synthetic oligonucleotides will be subcloned. CMV: cytomegalovirus promoter; SD: splice donor site; SA: splice acceptor site; RRE: Rev-responsive element; cPPT: central polypurine tract; CTS: central termination sequence; GFP: green fluorescent protein; PRE: woodchuck hepatitis virus post-transcriptional regulatory element. (b) RNAi effects by three siRNA HIV vectors for BRAF. The siRNAs #10 and #7′ are specific for wild-type BRAF mRNA, while siRNA #1′ is specific for mutated BRAF (V599E) mRNA. Western blot analysis of BRAF showed that siRNA #1′ decreased BRAF protein only in A375mel melanoma cell line with the mutated BRAF (V599E), but not in 293T cells without it, while siRNAs #10 and #7′ decreased the BRAF protein in both A375mel cells and 293T cells

RNAi effects of these BRAF siRNA HIV vectors were evaluated by infecting 293T cells (V599E mutation negative) and A375mel cells (V599E mutation positive) (Figure 1b). Decrease of the BRAF protein was observed in both the 293T embryonic kidney cell line and the A375mel melanoma cell line with both siRNA #10 and #7′, and was observed only in A375mel with siRNA #1′, indicating that the V599E mutation-directed siRNA #1′ is highly selective for the mutation.

Inhibition of MAP kinase activity and in vitro *proliferation of melanoma cell lines by BRAF RNAi*

To evaluate the effects of BRAF RNAi on various melanoma cell lines with or without the V599E mutation (Table 1), 10 melanoma cell lines including eight cell lines with the BRAF V599E mutation were infected with control GL3B (anti-firefly luciferase siRNA) or the BRAF siRNA (#10, #1′ or #7′)-expressing HIV vectors at 50 or 100 multiplicity of infection (MOI), then *in vitro* cell growth was evaluated by counting cell number every 3 days until day 6 or 9. No difference of transduction efficiency was observed among the melanoma cells infected with these siRNA vectors, since equivalent GFP expression (95–100%) was detected on the last culture day by flow cytometry.

siRNA #10 (and also #7′ in SKmel23), but not siRNA #1′, inhibited *in vitro* growth of SKmel23 and 1362mel melanoma cells, which did not have the V599E mutation (Figure 2a). The inhibition by two siRNAs targeting to different sequences of BRAF indicated that it is specifically caused by downregulation of BRAF. Western blot analysis (Figure 2b) demonstrated that siRNA #10 (and also #7′ in SKmel23), decreased the BRAF protein, while siRNA #1′ did not. siRNA #1′, however, inhibited growth of other eight melanoma cell lines with the V599E mutation to the same degree as siRNA #10

Table 1 Mutation status of BRAF (V599E) in melanoma cell lines used

Cell line	*Status of the BRAF mutation (V599E) in two alleles*
SKmel23	wt/wt
1362mel	wt/wt
A375mel	wt/mt
397mel	wt/mt
624mel	wt/mt
624Amel	wt/mt
526mel	wt/mt
888mel	wt/mt
928mel	wt/mt
1363mel	wt/mt

wt: wild-type BRAF; mt: BRAF with V599E mutation

except 624Amel for which all siRNAs were not effective (Figure 2c). siRNA #7′ was less inhibitory than siRNA #10 in seven melanoma cell lines (Figure 2a and c). Western blot analysis of the BRAF protein in the eight melanoma cell lines with the V599E mutation (Figure 2d) demonstrated that all siRNAs decreased the BRAF protein and suppressed phosphorylation of a downstream MAPK, ERK. On the other hand, normal primary fibroblasts were not affected by siRNA #1′ in terms of cellar growth and ERK phosphorylation levels (Figure 2e).

Interestingly, the *in vitro* cell growth correlated with the phosphorylation of ERK, but not with the BRAF protein level, when melanoma cells with V599E mutation were infected with siRNA #1′ (Figure 2c and d). The suppression of the ERK phosphorylation and cell growth inhibition by siRNA #1′ was equivalent to or even stronger than the siRNAs #10 and #7′, although the BRAF protein was less decreased by siRNA #1′ than by siRNA #10 or #7′ as observed in A375mel, 397mel, 526mel, 624mel, 1363mel and 888mel. This may be explained by 10–12-fold higher kinase activity of the mutated BRAF than wild-type BRAF as previously reported (Davies *et al*., 2002). To clarify the significance of the mutated BRAF on the MAPK signal pathway, we also evaluated wild-type-directed siRNA #1′ (wt) designed with the same region sequences as the mutation-directed siRNA #1′ (mt), and found a superior suppression with siRNA #1′ (mt) in the representative 526 mel melanoma cell line (Figure 2f). Most melanoma cell lines infected with the BRAF siRNA vectors eventually grow for 6 or 9 days after infection with the BRAF siRNA, although to a lesser degree than with the control vector (Figure 2a and c).

Clear cell death was observed in only 888mel among the 10 melanoma cell lines after infection with BRAF siRNA #10, #1′ and #7′, but not with control GL3B (Figure 2c). Apoptosis was not observed in 888mel, when dying 888mel was evaluated using DNA fragmentation assay by the agarose gel electrophoresis, and flow cytometric analysis with annexin V–FITC and propidium iodide (PI) (data not shown). 624Amel was the most resistant to the BRAF siRNAs among the 10 melanoma cell lines (Figure 2c). Although BRAF siRNA #10 and #7′ decreased the BRAF protein, ERK phosphorylation was not observed even with infection of the control GL3B, indicating a less important role of the BRAF–ERK pathway in the proliferation of 624Amel (Figure 2d).

BRAF RNAi leads to upregulation of ARAF and downregulation of MEK1

We next examined in more detail effects of BRAF RNAi on MAPK signaling pathways. Stimulation of the siRNA #10-infected 928mel with phorbol 12-myristate 13-acetate (PMA), which directly activates c-raf-1, only slightly increased ERK phosphorylation, which was less than we expected, possibly through activation of MEK (Figure 2a). To rule out inhibitory effect of BRAF RNAi on the downstream MAPK signaling, we evaluated other MAPK signaling molecules, including ARAF, c-raf-1, MEK1, MEK2, ERK1 and ERK2. Interestingly, upregulation of ARAF and downregulation of MEK1 were observed (Figure 3a). The same changes were also observed in A375mel transduced with BRAF siRNA #10, #1′ and #7′ (Figure 3b). Northern blot analysis did not show any difference in mRNA expression of ARAF and MEK1 among A375mel cells transduced with control GL3B, BRAF siRNA #10, #1′ or #7′ (Figure 3c), suggesting post-translational alternations. Although the mechanisms and effects of these ARAF and MEK1 changes should be investigated with further study, the BRAF–ERK pathway appears to function dominantly in melanoma cell proliferation, particularly with the BRAF mutation.

BRAF RNAi inhibited matrigel invasion of melanoma cells

Since MAP kinase pathways are also involved in tumor invasion, we have evaluated BRAF RNAi effects on the invasive ability of melanoma cell lines. A375mel and 928mel melanoma cell lines stably transduced with the control HIV lentivirus (GL3B) or three lentiviruses containing siRNAs against BRAF mRNA (siRNA #10, #1′ or #7′) were evaluated for *in vitro* invasive activity using a matrigel invasion assay. The number of cells passed across the matrigel layer was significantly reduced in A375mel and 928mel transduced with siRNA #10, #1′ or #7′, compared to siRNA GL3B (Figure 4a). The inhibition by three siRNAs targeting to the different BRAF sequences indicated that it was specifically mediated by the BRAF downregulation. The invasive activity may be inhibited through a decrease of matrix metalloproteinase (MMP)-2 activity and β_1 integrin that was observed when the invasion of A375mel cells was suppressed by infection with siRNA #10 (Figure 4b).

BRAF RNAi inhibited in vivo *tumorigenicity of melanoma*

We have then evaluated effects of the BRAF RNAi on *in vivo* melanoma growth, since melanoma cells whose proliferation was suppressed *in vitro* may still grow in *in vivo* microenvironment by other growth signals. A375mel cells were implanted subcutaneously in NOD/SCID mice, 2 days after *ex vivo* transduction with the BRAF siRNA HIV vectors or the control GL3B vector. At 24 days after the implantation, A375mel cells transduced with BRAF siRNA #10 or #1′ showed significantly reduced tumor growth compared to those with control GL3B (Figure 5) ($P<0.05$), suggesting that melanoma cells are highly dependent on the BRAF–ERK MAPK signaling pathway in *in vivo* growth. Considering these results of the *in vitro* and *in vivo* inhibition of proliferation and invasive ability, it is clear that the mutated BRAF is an excellent target for the treatment of melanoma.

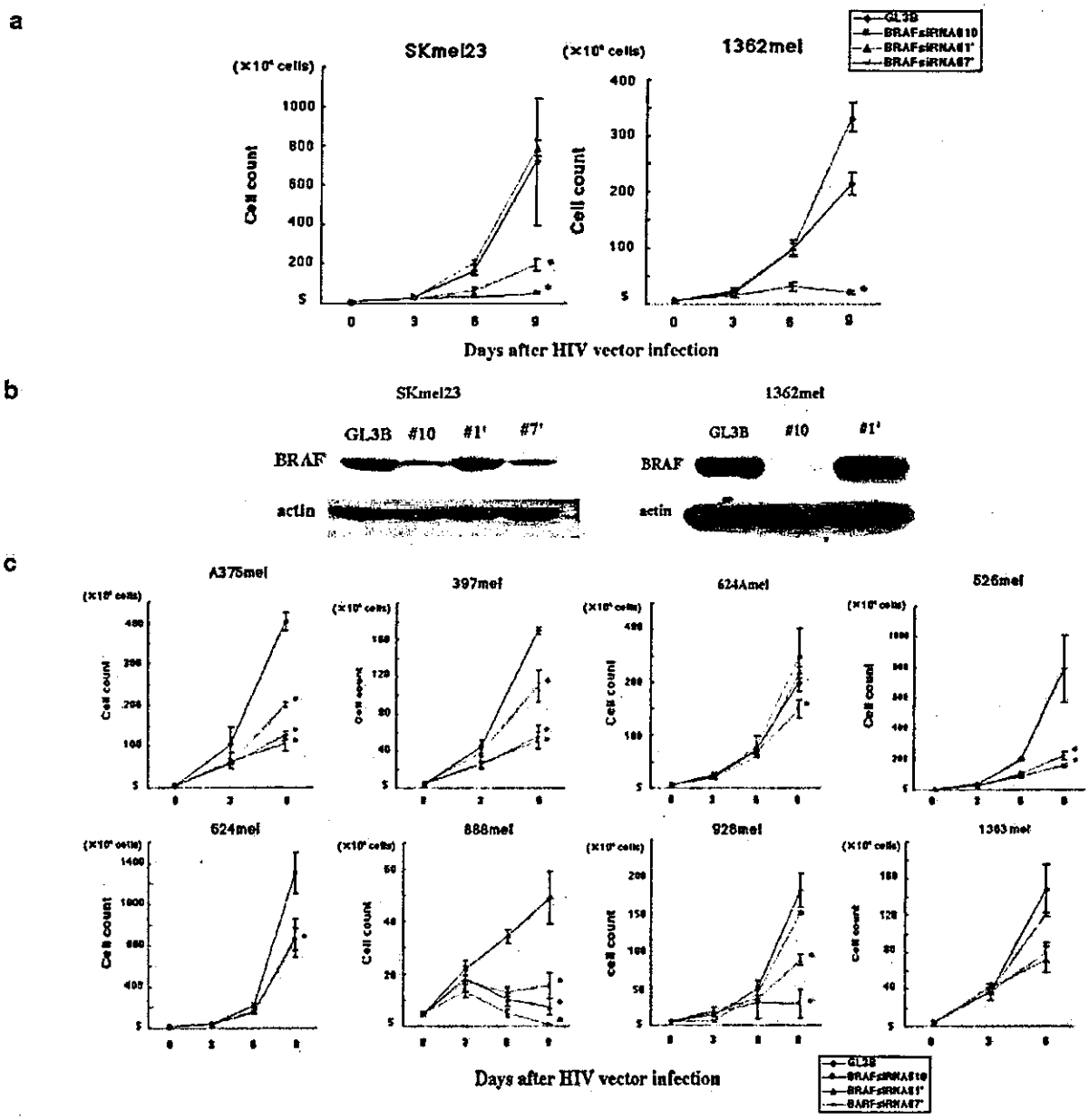
a
SKmel23
1362mel
(×10⁴ cells)
Cell count
GL3B
BRAFsiRNA#10
BRAFsiRNA#1'
BRAFsiRNA#7'
Days after HIV vector infection
b
SKmel23
1362mel
GL3B
#10
#1'
#7'
BRAF
actin
c
A375mel
397mel
624Amel
526mel
624mel
888mel
928mel
1363mel
Days after HIV vector infection
d
A375mel
397mel
624Amel
526mel
624mel
888mel
928mel
1363mel
BRAF
actin
ERK1
ERK2
ppERK1/2

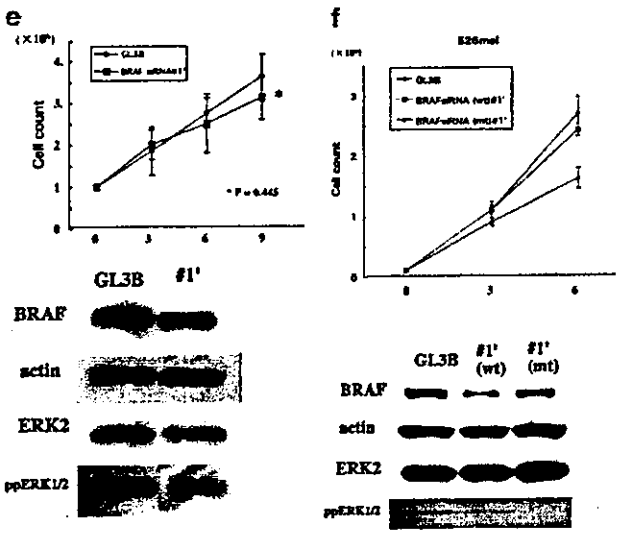

Figure 2 Continued

Discussion

We have developed siRNA-expressing HIV vectors for BRAF RNAi directed for either wild-type BRAF or the mutated BRAF (V599E) mRNA, which were detected in 66% of melanoma. Although both mutation-directed or nonspecific BRAF siRNA with lentiviral vectors led to a decrease of BRAF and ERK phosphorylation, and an inhibition of melanoma growth in most melanoma cell lines evaluated, reduction of ERK phosphorylation, but not BRAF, correlated well with cell growth inhibition, indicating that mutated BRAF, which has 10–12-fold more kinase activity than wild-type BRAF, is important for melanoma cell growth. This mutation-directed RNAi did not affect the normal fibroblast culture. Since the same inhibition was observed in *in vivo* melanoma growth, this study demonstrates that BRAF, particularly the V599E mutation, is an attractive molecular target for the treatment of melanoma.

Among the eight melanoma cell lines with the BRAF V599E mutation, different reactions following BRAF RNAi were observed. Marked cell death by necrosis, but not by apoptosis, was seen in only 888mel. It may be because of unknown signaling difference in 888mel. Since copy numbers obtained by lentiviral vector transduction are relatively limited, use of higher expression system may result in different cellular outcomes such as induction of more cell death and apoptosis. Recently, Hingorani *et al.* (2003) reported that inhibition of BRAF (V599E) by using a plasmid vector expressing siRNA in one melanoma cell line, WM793, resulted in growth arrest and apoptosis *in vitro*, which was detected by TUNEL assay of a stable siRNA transfectant. Their results differ from ours in that induction of cell death was not in general and apoptosis was not found by inhibition of the BRAF–MAPK pathway. Since their report was based on only one cell line, more extensive investigation is necessary for the confirmation of apoptosis induction with high-copy RNAi systems.

624Amel with the V599E mutation is resistant to both the mutation-directed and nonspecific BRAF RNAi. Although ERK phosphorylation was detectable in most melanoma cell lines in usual culture condition, it was not detected in 624Amel. Activation of the BRAF–ERK pathway appears not to be important for 624Amel. The fact that the parent melanoma cell line, 624mel, was relatively sensitive for BRAF RNAi may suggest heterogeneity of tumor cell clones or the genetic changes relating to the suppression of the BRAF–MAPK pathway during cell proliferation. It should be noted that BRAF may not be critical for cell proliferation of even melanoma cells with the V599E mutation. 624mel has a mutation in phosphorylation sites (S45Y) in β-catenin, resulting in increased expression of β-catenin protein through poor degradation in proteosomes (Rubinfeld *et al.*, 1997). Thus, activation of the Wnt signal pathway is one candidate for complement proliferation of melanoma in 624mel. However, proliferation of 888mel having a mutation of another phosphorylation site of β-catenin (S37F) (Robbins *et al.*, 1996) was strongly inhibited accompanied by cell death. Thus, the mechanism of the resistance of 624mel to BRAF RNAi remains to be further investigated and it will provide important insights for resistance of melanoma in the future anti-BRAF treatment.

MMPs are a family of proteases that are involved in matrix remodeling. Particularly, MMP-2 is involved in tumor cell invasion by degradation of basement membrane collagen (Puyraimond *et al.*, 1999). The MMP-2 expression was reported to be a poor prognostic factor for patients with melanoma (Vaisanen *et al.*,

Figure 2 Inhibition of *in vitro* melanoma growth accompanied by decrease of the BRAF protein and ERK phosphorylation. (a) Inhibition of *in vitro* growth of SKmel23 and 1362mel melanoma cell lines without the BRAF (V599E) mutation was evaluated by counting cultured cells. (b) Decrease of the BRAF protein was detected by Western blot analysis, by infection with wild-type BRAF-specific RNAi vectors, siRNA #10 and #7′, but not by the V599E mutation-specific RNAi. (c) Inhibition of *in vitro* growth of eight melanoma cells with the BRAF (V599E) mutation by BRAF RNAi. Growth of the melanoma cells except 624Amel was reduced by infection with siRNA #1′. 624Amel was resistant to all siRNA vectors. (d) Western blot analysis of the BRAF–MAPK cascade in eight melanoma cells indicated in (c). BRAF protein was reduced to a lesser extent with siRNA #1′ than with siRNA #10 or #7′; however, ERK phosphorylation (ppERK) was reduced to a greater extent with siRNA #1′ than with siRNA #10 or #7′. Inhibition of melanoma growth correlated well with the reduction of ppERK, suggesting greater involvement of the mutated BRAF in melanoma cell proliferation. (a) and (c) show one representative result for each cell line from two or three experiments performed. Error bars indicate standard deviations. $^*P<0.05$. (e) Effects of BRAF siRNA #10 and #1′ on the *in vitro* cell growth and MAPK pathway of human primary fibroblasts. The siRNA #1′ did not affect both *in vitro* cell growth and ERK phosphorylation. (f) Comparison of siRNAs specific for the wild-type BRAF and the mutation-specific BRAF in 526mel. The siRNA (mt)#1′ suppressed both *in vitro* growth and ERK phosphorylation more than the siRNA (wt)#1′. (Percentage of GFP-positive cells: GL3B 98.6%, siRNA (wt)#1′ 99.9%, siRNA (mt)#1′ 85.9%)

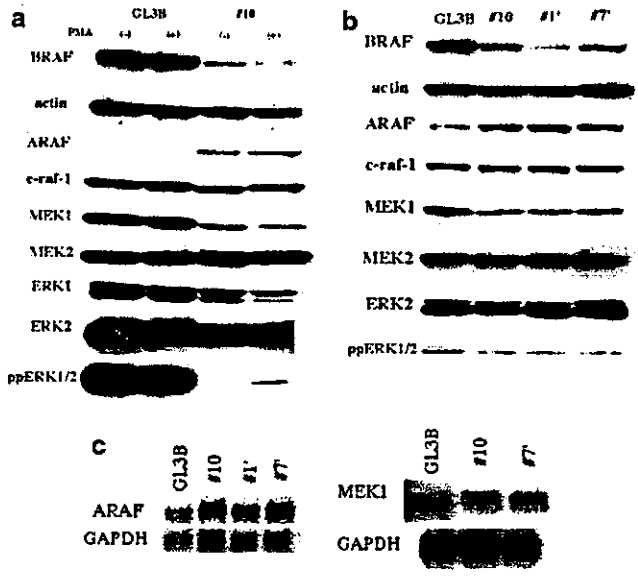

Figure 3 Increase of ARAF protein and decrease of MEK1 protein with no altered mRNA expression after BRAF RNAi. (a) Western blot analysis of proteins involved in the MAPK pathway in 928mel melanoma cell line after BRAF RNAi with or without PMA stimulation. PMA slightly restored the ERK phosphorylation of 928mel cells after BRAF RNAi. Decrease of the BRAF protein by siRNA #10 was associated with the increase of the ARAF protein and the decrease of the MEK1 protein. (b) Western blot analysis of proteins involved in the MAPK pathway in A375mel melanoma cell line after BRAF RNAi. Decrease of the BRAF protein by siRNA #10, #1′ and #7′ was associated with the increase of the ARAF protein and the decrease of the MEK1 protein. (c) Northern blot analysis of ARAF and MEK1 in A375mel melanoma cell line after BRAF RNAi. Expressions of both ARAF and MEK1 mRNA were not different among A375mel infected with the control GL3B siRNA and BRAF siRNAs, indicating that the protein changes shown in (b) were post-translational

1999). The expression of MMPs is regulated by ERK1/2 (Aguirre Ghiso *et al*., 1999; Genersch *et al*., 2000; Santibanez *et al*, 2000). Integrins are involved in metastasis of melanoma through their interaction with the extracellular matrix (ECM) components (Hynes, 1992). The expression of $\alpha_3\beta_1$ integrins is important for adhesion of melanoma cells to dermal collagen as well as for prevention of apoptosis and is reported to be a prognostic factor for melanoma patients (Natali *et al*., 1993; Melchiori *et al*., 1995). Integrins also trigger cell signalings participating in cell cycle progression and survival (Montgomery *et al*., 1994; Petitclerc *et al*., 1999). The MAPK cascade is also involved in the expression of β integrins (Woods *et al*., 2001). Therefore, the decrease of matrigel invasion accompanied by a decrease of MMP activity and β_1 integrins possibly through the suppression of the MAP kinase activity by BRAF RNAi, demonstrated in this study (Figures 2d, 3a and b), indicates important roles of BRAF in invasion and metastasis of melanoma, indicating that BRAF is an attractive target for inhibition of melanoma spread.

When we evaluated ERK phosphorylation after overnight serum starvation, it was detected in only three melanoma cell lines, A375mel, 397mel and 526mel, of total eight melanoma cell lines tested (data not shown). The constitutive activation of the MAPK pathway by the mutated BRAF may not be so high as suggested by a previous report (Satyamoorthy *et al*., 2003). No correlation was observed between detectable constitutive activation of ERK and the inhibitory effects on melanoma growth by BRAF RNAi. In this study, we unexpectedly observed an increase of ARAF and a decrease of MEK1 protein after BRAF RNAi. These changes appear to be post-translationally regulated, since no different mRNA expression was seen by Northern blot analysis. Changes of stability or degradation of these proteins may be regulated by the BRAF–MAPK pathway.

In summary, this study for the first time clarified the important roles of the mutated BRAF in melanoma proliferation *in vivo* as well as invasion and metastasis. Therefore, molecular target therapy using BRAF kinase inhibitors or gene therapy directed for mutated BRAF should be vigorously investigated for future clinical use. Since an efficient *in vivo* gene transduction will be required for RNAi to activated oncogenes in cancer gene therapy, we are now trying to establish a more highly transducible vector system by using adenoviral vectors.

Methods

Cell lines

Melanoma cell lines, 397mel, 526mel, 624mel, 624Amel, 888mel, 928mel, 1362mel and 1363mel, were generated in the Surgery Branch, National cancer Institute, National Institutes of Health, Bethesda, MD, USA, and generously provided by Dr Steven A Rosenberg (Kawakami *et al*., 1994). A375mel was purchased from American Type Culture Collection (ATCC, Manassas, VA, USA). Skmel23 was kindly provided by Dr T Boon, Ludiwig Institute for Cancer Research and Cellular Genetics Unit, Brussels, Belgium). These cell lines were cultured in RPMI 1640 medium supplemented with 10% FCS. Human primary fibroblasts obtained from a healthy volunteer were cultured in DMEM supplemented with 10% FCS.

HIV-U6i-GFP plasmid

The siRNA expression unit containing human U6 promoter and two *Bsp*MI sites was subcloned between CTS and GFP expression unit in an HIV vector plasmid, which is a self-inactivating (SIN) vector lacking its own promoter sequence in the 3′-LTR, enabling GFP expression under the control of internal CMV promoter, carrying central polypurine tract (cPPT) and woodchuck hepatitis virus post-transcriptional regulatory element (PRE) for enhanced nuclear transport of the transcribed mRNA. A series of siRNA expression plasmids were constructed based on the HIV-U6i-GFP plasmid (Figure 1a).

HIV vectors

Three siRNA target sequences were selected for BRAF RNAi: (1) siRNA #10 GTATCACCATCTCCATATCAT; (2) (mt)

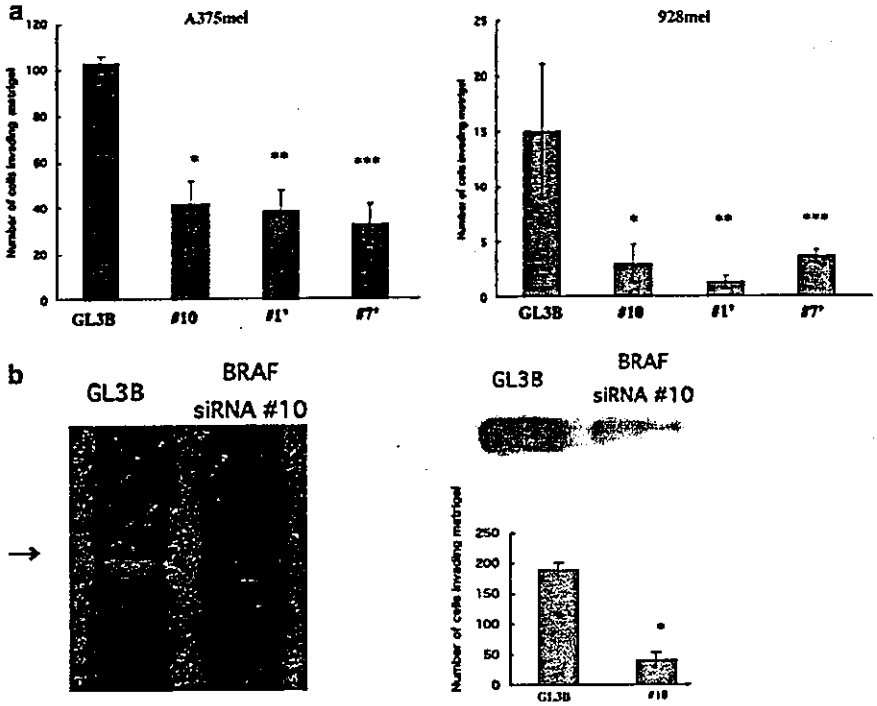

Figure 4 Inhibition of melanoma cell invasion in matrigel by BRAF RNAi. (**a**) Inhibition of invasion of melanoma cell lines by BRAF RNAi. Matrigel invasion ability of A375mel and 928mel melanoma cell lines was inhibited by three different siRNAs. A total of 25 000 melanoma cell lines transduced with the lentiviral vectors (GL3B, #10, #1′ and #7′) were plated on the matrigel invasion chambers and cultured. After 24 h, the number of migrated cells that adhered to the bottom surface of the chamber was counted. The vertical bars indicate s.d. of triplicate assays. Left: A375, $*P=0.0006$, $**P=0.0003$, $***P=0.0002$. Right: 928mel, $*P=0.0303$, $**P=0.0179$, $***P=0.0325$. (**b**) Decrease of MMP-2 activity and β_1 integrin in A375mel whose invasion in matrigel was suppressed by BRAF siRNA. Left: Decrease of MMP-2 activity by BRAF RNAi evaluated with gelatin zymograpy. The cell lysates from A375mel/GL3B and A375mel/BRAF siRNA #10 were electrophoresed in an SDS–PAGE gel containing 0.2% gelatin. After incubation of the gel in TNC buffer, the gel was stained in CBB and visualized for the gelatinolysed area. The arrow indicates gelatinolysed area corresponding to 75 kDa MMP-2. Upper right: Decrease of β_1 integrin evaluated with Western blot analysis. The cell lysates from A375mel/GL3B and A375mel/BRAF siRNA #10 were blotted with anti-β_1-integrin antibody. Lower right: Inhibition of matrigel invasion of A375mel by BRAF RNAi #10. $*P=0.0001$

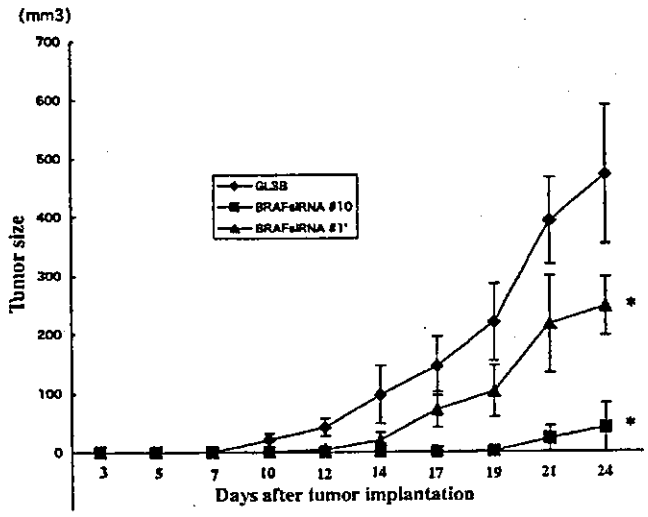

Figure 5 BRAF RNAi reduced *in vivo* tumorigenicity of melanoma cells. NOD/SCID mice (6-week-old) were implanted s.c. with 5×10^5 A375mel cells infected with lentiviral vectors expressing siRNA for firefly luciferase (GL3B), BRAF #10 or BRAF #1′. The tumor volume was measured every 2–3 days until day 24. $*P<0.05$. The vertical bars indicate standard deviation. $n=5$. This experiment is representative of three independent experiments with the same results

siRNA #1′ GCTACAGAGAAATCTCGAT; (3) (wt) siRNA #1′ GCTACAGTGAAATCTCGAT and (4) siRNA #7′ GCCACAACTGGCTATTGTTA. Two complementary oligonucleotides, cacc-(target sense)-TTCAAGA-GA-(target antisense)-TTTTT and gcatAAAAA-(target sense)-TCTCTTGAA-(target antisense), were synthesized for each target sequence and annealed *in vitro*. The annealed double-stranded (ds) oligonucleotides with 5′-protruding ends complementary to the two *Bsp*MI sites in the HIV-U6i-GFP plasmid were then subcloned into HIV-U6i-GFP. Control GL3B siRNA (anti-firefly luciferase siRNA) HIV vector was also constructed with the target sequence GTGCGCTGCTGGTGCCAAC. These HIV vectors would produce short hairpin RNA with the linker sequence (TTCAAGAGA) forming a loop structure, then the linker would be processed by Dicer, forming a dsRNA, which acts as an siRNA. The third-generation HIV vectors were produced by transfecting 293T cells with HIV plasmid vectors, pMD.G (VSV-G env expression plasmid), pMDLg/p.RRE (the third-generation packaging plasmid) and pRSV Rev (Rev expression plasmid) (the latter two plasmids were provided by Cell Genesys, USA), by calcium phosphate transfection. The culture supernatant was collected and used as the virus stock after concentration. The viral titer was measured by infecting 293T cells and evaluating GFP expression.

In vitro *growth inhibition assay of melanoma cells by BRAF RNAi*

A total of 10 melanoma cell lines were first analysed for the presence of the BRAF V599E mutation by direct sequencing of the RT–PCR product from the melanoma RNAs. The PCR conditions were as follows: forward primer GGCTCCAGC TTGTATCACCATCTCC, reverse primer CAGGTATCC TCGTCCCAC CATAAAA, hot started at 94°C for 5 min, followed by 30 cycles of denaturing at 94°C for 1 min, annealing at 55°C for 1 min and extension at 72°C for 1 min, followed by final extension at 72°C for 7 min. A total of 10 melanoma cell lines, including eight cell lines with BRAF V599E (1363mel, A375mel, 397mel, 501Amel, 526mel, 624mel, 928mel and 888mel) and two cell lines without BRAF V599E (Skmel23 and 1362mel), were infected with the BRAF siRNA-expressing HIV vectors at 50 or 100 MOI at day 0. Cell numbers were counted every 3 days by Trypan blue dye exclusion method until day 6 or 9. The siRNA HIV vector for firefly luciferase (GL3B) was used as a control. Human primary fibroblasts were infected and evaluated as melanomas as a control.

Western blot analysis for proteins involved in MAPK pathway and β_1 integrin after BRAF RNAi in melanomas

Cell lysates were prepared in the lysis buffer (20 mM Tris-HCl (pH 7.5), 12.5 mM β-glycerophosphate, 2 mM EGTA, 10 mM NaF, 1 mM benzamide, 1% NP-40, protease inhibition cocktail (complete, EDTA-free (Roche, Germany)) and 1 mM Na_3VO_4) from the infected melanoma cells used in *in vitro* growth inhibition assay after confirmation of equivalent GFP expression among the control and BRAF RNAi-infected cells by flow cytometry. The protein concentration was determined by the DC protein assay kit (Bio-Rad, USA). Anti-BRAF (Santa Cruz, USA), anti-actin (Sigma, USA), anti-ERK1 (Santa Cruz, USA), anti-ERK2 (Santa Cruz, USA), or anti-ppERK1/2 (Cell Signaling, USA), anti-ARAF (Becton-Dickinson, USA), anti-c-raf-1 (Becton-Dickinson, USA), anti-MEK1 (Becton-Dickinson, USA), anti-MEK2 (Santa Cruz, USA) and β1 integrin (BD Transduction, USA) Abs were used as the first antibodies. HRP-conjugated anti-IgG antibodies were used as the second antibodies and the reaction was detected by chemiluminescence with SuperSignal West Femto Maximum Sensitivity Substrate (Pierce, USA). 928mel cells transduced with HIV vectors expressing GL3B or BRAF siRNA #10 were treated with PMA (Sigma, USA) at a final concentration of 100 nM. The cell lysates were prepared 15 min after the treatment for Western blot analysis.

Northern blot anaylsis

Total RNAs were prepared from A375mel cells transduced with HIV vectors expressing GL3B and BRAF siRNA #10, #1′ or #7′ by using TRIzol (Invitrogen, USA). A 10 μg measure of each total RNA was fractionated by formaldehyde-containing agarose gel electrophoresis, and then transferred to a nylon membrane (Hybond-XL; Amersham Pharmacia, USA). Radioisotope-labeled ARAF, MEK-1 or GAPDH cDNA fragments were generated using the High Prime DNA Labeling Kit (Boehringer Mannheim, Germany). Prehybridization and hybridization with the radioisotope-labeled cDNA fragments were performed using Quick Hyb solution (Stratagene, USA). Radioactive signals were detected using BAS-5000 (Fuji Film, Japan).

Animal experiments

Female NOD/SCID mice (6-week-old) (Japan CLEA, Japan) were subcutaneously implanted with half a million of A375mel melanoma cell line transduced with HIV vectors expressing GL3B, BRAF siRNA #10 or #1′ ($n=5$). The tumor volume (largest diameter × perpendicular diameter × height) was measured every 2–3 days until day 24. The animal experimental protocol was approved by the Laboratory Animal Care and Use Committee at Keio University School of Medicine. Mice were treated according to the Guidelines for the Care and Use of Laboratory Animals of Keio University School of Medicine.

Matrigel invasion assay A375mel or 928mel melanoma cells transduced with siRNA GL3B, #10, #1′ or #7′ were plated in BioCoat Matrigel invasion chambers (Becton-Dickinson, MA, USA) at a cell density of 2.5×10^4 cells/chamber and incubated at 37°C and 5% CO_2 for 24 h. After the incubation, noninvading cells remaining on the upper surface of the chamber were removed by scrubbing with a cotton-tipped swab and the invaded cells adhering to the bottom surface of the chamber membrane were fixed and counted after cell staining with Diff-Quik stain (Sysmex, Kobe, Japan) according to the manufacturer's instructions.

Gelatin zymography

A 30 μg measure of cell lysates from A375mel/GL3B or A375mel/BRAF siRNA #10 was electrophoresed in an SDS–PAGE gel containing 0.2% gelatin. The gel was rinsed in 2.5% Triton X-100 for 15 min twice, followed by incubation in TNC buffer (10 mM Tris-HCl (pH 7.5), 150 mM NaCl and 10 mM $CaCl_2$) at 37°C for 24 h. The gel was stained in Coomassie brilliant blue (CBB) for 30 min and the unstained band was visualized.

Statistical analysis

All statistical analyses were performed according to unpaired Student *t*-test.

Acknowledgements
We thank Dr Matsuda for helpful advices and critical review of the manuscript and Drs Okada and Shiomi for helpful advices. This work was supported in part by research grants from the Ministry of Education, Culture, Sports, Science and Technology, research grants from the Ministry of Health, Labour and Welfare and Keio Gijuku Academic Development Funds.

References

Abbas-Terki T, Blanco-Bose W, Deglon N, Pralong W and Aebischer P. (2002). *Hum. Gene Ther.*, **13**, 2197–2201.

Aguirre Ghiso JA, Kovalski K and Ossowski L. (1999). *J. Cell Biol.*, **147**, 89–104.

Barton GM and Medzhitov R. (2002). *Proc. Natl. Acad. Sci. USA*, **99**, 14943–14945.

Bernstein E, Caudy AA, Hammond SM and Hannon GJ. (2001). *Nature*, **409**, 363–366.

Brummelkamp TR, Bernards R and Agami R. (2002a). *Science*, **296**, 550–553.

Brummelkamp TR, Bernards R and Agami R. (2002b). *Cancer Cell*, **2**, 243–247.

Cobb MH. (1999). *Prog. Biophys. Mol. Biol.*, **74**, 479–500.
Davies H, Bignell GR, Cox C, Stephens P, Edkins S, Clegg S, Teague J, Woffendin H, Garnett MJ, Bottomley W, Davis N, Dicks E, Ewing R, Floyd Y, Gray K, Hall S, Hawes R, Hughes J, Kosmidou V, Menzies A, Mould C, Parker A, Stevens C, Watt S, Hooper S, Wilson R, Jayatilake H, Gusterson BA, Cooper C, Shipley J, Hargrave D, Pritchard-Jones K, Maitland N, Chenevix-Trench G, Riggins GJ, Bigner DD, Palmieri G, Cossu A, Flanagan A, Nicholson A, Ho JWC, Leung SY, Yuen ST, Barbara LW, Seigler HF, Darrow TL, Paterson H, Marais R, Marshall CJ, Wooster R, Stratton MR and Futreal PA. (2002). *Nature*, **417**, 949–954.
Devroe E and Silver PA. (2002). *BMC Biotechnol.*, **28**, 15.
Elbashir SM, Harborth J, Lendeckel W, Yalcin A, Weber K and Tuschl T. (2001). *Nature*, **411**, 494–498.
Genersch E, Hayess K, Neuenfeld Y and Haller H. (2000). *J. Cell Sci.*, **113**, 521–530.
Hannon GJ. (2002). *Nature*, **418**, 244–251.
Hingorani SR, Jacobetz MA, Robertson GP, Herlyn M and Tuveson DA. (2003). *Cancer Res.*, **63**, 5198–5202.
Hynes RO. (1992). *Cell*, **69**, 11–25.
Kawakami Y, Eliyahu S, Delgado CH, Robbins PF, Rivoltini L, Topalian SL, Miki T and Rosenberg SA. (1994). *Proc. Natl. Acad. Sci. USA*, **91**, 3515–3619.
Kawasaki H and Taira K. (2003). *Nucleic Acids Res.*, **31**, 700–707.
Lee NS, Dohjima T, Bauer G, Li H, Li MJ, Ehsani A, Salvaterra P and Rossi J. (2002). *Nat. Biotechnol.*, **19**, 500–505.
Melchiori A, Mortarini R, Carlone S, Marchisio PC, Anichini A, Noonan DM and Albini A. (1995). *Exp. Cell Res.*, **219**, 233–242.
Miyagishi M and Taira K. (2002). *Nat. Biotechnol.*, **19**, 497–500.
Miyagishi M, Sumimoto H, Miyoshi H, Kawakami Y and Taira K. *J. Gene Med.* (in press).
Montgomery AM, Reisfeld RA and Cheresh DA. (1994). *Proc. Natl. Acad. Sci. USA*, **91**, 8856–8860.
Natali PG, Nicotra MR, Bartolazzi A, Cavaliere R and Bigotti A. (1993). *Int. J. Cancer*, **54**, 68–72.
Paddison PJ, Caudy AA, Bernstein E, Hannon GJ and Conklin DS. (2002). *Genes Dev.*, **16**, 948–958.
Paul CP, Good PD, Winer I and Engelke DR. (2002). *Nat. Biotechnol.*, **19**, 505–508.
Petitclerc E, Stromblad S, von Schalscha TL, Mitjans F, Piulats J, Montgomery AM, Cheresh DA and Brooks PC. (1999). *Cancer Res.*, **59**, 2724–2730.
Puyraimond A, Weitzman JB, Babiole E and Menashi S. (1999). *J. Cell Sci.*, **112**, 1283–1290.
Qin XF, An DS, Chen ISY and Baltimore D. (2003). *Proc. Natl. Acad. Sci. USA*, **100**, 183–188.
Robbins PF, El-Gamil M, Li YF, Kawakami Y, Loftus D, Apella E and Rosenberg SA. (1996). *J. Exp. Med.*, **183**, 1185–1192.
Rubinfeld B, Robbins P, El-Gamil M, Albert I, Porfiri E and Polakis P. (1997). *Science*, **275**, 1790–1792.
Rubinson DA, Dillon CP, Kwiatkowski AV, Sievers C, Yang L, Kopinja J, Zhang M, McManus MT, Gertler FB, Scott ML and Parijs LV. (2003). *Nat. Genet.*, **33**, 401–406.
Santibanez JF, Iglesias M, Frontelo P, Martinez J and Quintanilla M. (2000). *Biochem. Biophys. Res. Commun.*, **273**, 521–527.
Satyamoorthy K, Li G, Gerrero MR, Brose MS, Volpe P, Weber BL, Belle PV, Elder DE and Herlyn M. (2003). *Cancer Res.*, **63**, 756–759.
Smalley KSM. (2003). *Int. J. Cancer*, **104**, 527–532.
Sui G, Soohoo C, Affar EB, Gay F, Shi Y, Forrester WC and Shi Y. (2002). *Proc. Natl. Acad. Sci. USA*, **99**, 5515–5520.
Tiscornia G, Singer O, Ikawa M and Verma IM. (2003). *Proc. Natl. Acad. Sci. USA*, **100**, 1844–1848.
Tuschl T. (2002). *Nat. Biotechnol.*, **20**, 446–448.
Vaisanen A, Kallioinen M, von Dickhoff K, Laatikainen L, Hoyhtya M and Turpeenniemi-Hujanen T. (1999). *J. Pathol.*, **188**, 56–62.
Woods D, Cherwinski H, Venetsanakos E, Bhat A, Gysin S, Humbert M, Bray PF, Saylor VL and McMahon M. (2001). *Mol. Cell. Biol.*, **21**, 3192–3205.
Xia H, Mao Q, Paulson HL and Davidson BL. (2002). *Nat. Biotechnol.*, **20**, 1006–1010.
Yu JY, DeRuiter SL and Turner DL. (2002). *Proc. Natl. Acad. Sci. USA*, **99**, 6047–6052.

doi:10.1016/j.ymthe.2004.05.006

Adenovirus-Mediated Transfer of siRNA against Survivin Induced Apoptosis and Attenuated Tumor Cell Growth *in Vitro* and *in Vivo*

Hiroaki Uchida,[1,2] Toshihiro Tanaka,[1] Katsunori Sasaki,[1] Kazunori Kato,[1] Hironari Dehari,[1] Yoshinori Ito,[1] Masayoshi Kobune,[1,3] Makoto Miyagishi,[4] Kazunari Taira,[4] Hideaki Tahara,[2] and Hirofumi Hamada[1,*]

[1] *Department of Molecular Medicine, Sapporo Medical University, Sapporo 060-8556, Japan*
[2] *Department of Surgery and Bioengineering, Institute of Medical Science, The University of Tokyo, Tokyo 108-8639, Japan*
[3] *Fourth Department of Internal Medicine, Sapporo Medical University, Sapporo 060-8556, Japan*
[4] *Department of Chemistry and Biotechnology, School of Engineering, The University of Tokyo, Tokyo 113-8656, Japan*

**To whom correspondence and reprint requests should be addressed at the Department of Molecular Medicine, Sapporo Medical University, South-1, West-17, Chuo-ku, Sapporo 060-8556, Japan. Fax: +81-11-611-2136. E-mail: hhamada@sapmed.ac.jp.*

Gene targeting using short interfering RNA (siRNA) has become a common strategy to explore gene function because of its prominent efficacy and specificity. For the application of siRNA technology to gene therapy, however, still more efficient transduction of siRNA into target cells is needed. In this study, we developed an adenoviral vector harboring a tandem-type siRNA expression unit, in which sense and antisense strands composing the siRNA duplex were separately transcribed by two human U6 promoters. Targeting survivin, an antiapoptotic molecule widely overexpressed in malignancies but not detected in terminally differentiated adult tissues, this type of adenoviral vector (Adv-siSurv) successfully exerted a gene knockdown effect and induced apoptosis in HeLa, U251, and MCF-7 cells. These cancer cells, once infected with Adv-siSurv, displayed remarkably attenuated growth potential, both *in vitro* and *in vivo*. Moreover, intratumoral injection of Adv-siSurv significantly suppressed tumor growth in a xenograft model using U251 glioma cells. This novel modality may be a promising tool for cancer therapy.

Key Words: short interfering RNA, adenoviral vector, cancer gene therapy, survivin, apoptosis

Introduction

RNA interference (RNAi) is a process of posttranscriptional gene silencing in which double-stranded RNA (dsRNA) inhibits gene expression in a sequence-dependent manner via degradation of the corresponding mRNA [1–4]. RNAi is initiated by an event whereby dsRNAs are recognized by Dicer, a member of the RNase III protein family [5]. The Dicer enzyme cleaves dsRNAs into 21- to 23-nucleotide (nt) short interfering RNAs (siRNAs). These siRNA duplexes are incorporated into a protein complex called the RNA-induced silencing complex, which recognizes and cleaves the cognate mRNA [6,7]. Recently, Tuschl and his colleagues have reported that introduction of synthetic 21-nt siRNA into mammalian cells suppressed gene expression in a sequence-specific manner [8]. By using dsRNAs of such a small size, the activation of dsRNA-dependent protein kinase and 2′,5′-oligoadenylate synthetase, which occurs as an interferon response to long dsRNA (i.e., longer than 30 nt), leading to a global decrease in protein synthesis, was avoided [9,10]. Thus, siRNA has now become a routine tool for studies of gene function in basic research. However, to facilitate the application of siRNA in cancer gene therapy approaches, improved methods for efficient introduction of siRNA into target cells should be developed. Several groups, including ours, have reported the efficacy of vector-based siRNA expression systems in which siRNAs are transcribed by either the U6 or the H1 promoter [11–19]. Nevertheless, since not all cancer cell types are susceptible to transfection of plasmid DNA, there is a need for the development of recombinant viral vectors to facilitate expression of siRNAs for potential use in cancer gene therapy applications.

1525-0016/$30.00

The inhibitor of apoptosis protein (IAP) family is characterized by the presence of one or more baculovirus IAP repeat (BIR) domains. IAP family members are known to prevent caspase activation by interacting with caspases via these domains, thereby inhibiting apoptosis induced by various stimuli [20–23]. Survivin, a member of the IAP family, differs from the other members, including cellular IAP (cIAP)-1, cIAP-2, and X-linked IAP (XIAP), in several aspects [24]. Structurally, survivin contains a single BIR domain and lacks a RING-finger motif. Survivin has been shown to be a bifunctional protein that regulates cell division and suppresses apoptosis [24–27]. Most importantly in the context of cancer therapy, survivin is expressed in most cancers and during embryonic and fetal development, but is largely undetectable in terminally differentiated adult tissues [24,28,29]. Therefore, survivin is considered to be an attractive target with respect to molecular therapy of cancer. Functional interference with survivin using a dominant-negative mutant, survivin (T34A), has been shown to induce apoptosis in tumor cells both *in vitro* and *in vivo* [30]. Attenuation of survivin expression using antisense oligonucleotides or ribozymes has been also shown to induce apoptosis in cancer cells and sensitize cancer cells to anticancer agents [31–34].

In this study, we designed recombinant adenoviral vectors encoding siRNA against survivin and investigated their efficacy in regard to suppression of survivin expression in cancer cells and consequent antitumor potential.

Results

Transfection of Plasmid DNA Encoding U6 Promoter-Driven siRNA against Survivin Strongly and Specifically Suppressed Survivin Expression in 293T Cells

We constructed two kinds of plasmid vectors encoding human U6 promoter-driven siRNAs against different target sites within the survivin transcript, psiSurv(A) and psiSurv(B). We transfected these survivin-oriented siRNA-expressing plasmids, as well as control plasmids, separately into 293T cells by lipofection. Seventy-two hours later, we estimated the expression level of survivin in the transfected cells. RT-PCR analysis revealed that lipofection of either of the survivin-oriented siRNA-expressing plasmids into 293T cells led to remarkable suppression of survivin mRNA expression compared to transfection of the control plasmid pUC19 or psiGL3B (Fig. 1A). Similarly, immunoblot analysis showed that the expression of survivin protein in 293T cells transfected with the survivin-oriented siRNA-expressing plasmids was strongly inhibited (Fig. 1B). Densitometric analysis revealed that the amount of survivin protein remaining in cells transfected with psiSurv(A) and psiSurv(B) was 12 and 37%, respectively, of that found in cells transfected with pUC19, a control plasmid devoid of an siRNA expression

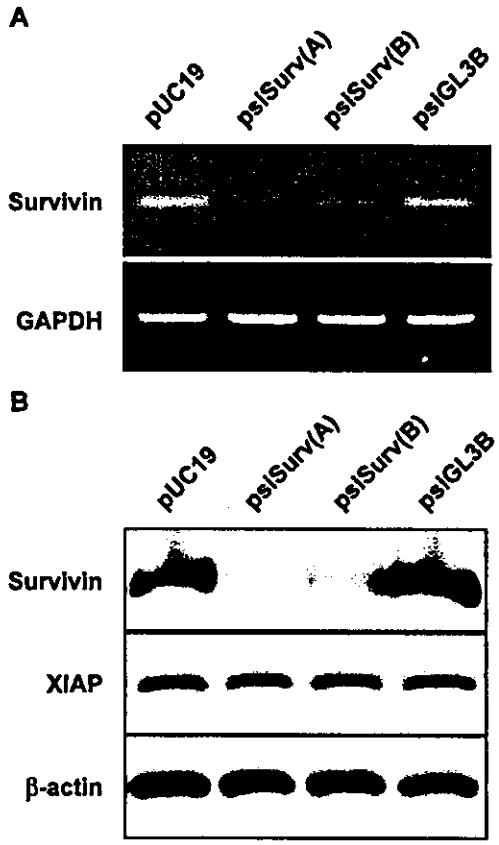

FIG. 1. The effects of plasmid vectors encoding U6 promoter-driven siRNA against survivin on survivin expression in 293T cells. 293T cells (8×10^5) were seeded onto 60-mm dishes. Sixteen hours later, the seeded cells were transfected with 6 μg DNA by lipofection. (A) RT-PCR analysis of survivin or GAPDH (internal control) mRNA expression performed 72 h after transfection. (B) Immunoblot analysis of survivin, XIAP, or β-actin (internal control) protein expression performed 72 h after transfection. pUC19 and psiGL3B are control vectors encoding either no expression unit or siRNA against firefly luciferase. psiSurv(A) and psiSurv(B) are the vectors that express siRNA against different sites of the survivin transcript. The survivin levels remaining were calculated as % control relative to loading control.

cassette. Transfection of psiGL3B, a control vector expressing siRNA against the firefly luciferase transcript, had no impact on survivin expression at either the mRNA or the protein level (Figs. 1A and 1B). Importantly, transfection of neither psiSurv(A) nor psiSurv(B) affected the expression level of XIAP, another member of the IAP family (Fig. 1B). Taken together, these plasmid vectors expressing siRNAs against survivin exerted a powerful and specific knockdown effect with respect to endogenous survivin expression in 293T cells.

Adenovirus-Mediated Transduction of siRNA against Survivin Suppressed Survivin Expression in Cancer Cells

293T cells are one of the most frequently used cell lines in transfection studies because of the excellent trans-

duction efficiency of plasmid DNA. However, many types of cancer cells are much less susceptible to plasmid DNA transfection compared to 293T cells. Thus, we designed analogous recombinant adenoviruses encoding siRNA that also targeted the survivin transcript (Adv-siSurv(A) and Adv-siSurv(B)). The structure of these adenoviral vectors is shown in Fig. 2. The backbone of the adenoviral vectors used in this study was an E1- and E3-deleted serotype 5 adenovirus with a modified fiber F/RGD, harboring an integrin-binding RGD motif within the HI loop of its knob protein, for improvement of gene transfer efficiency. The target sites within the survivin transcript of both the plasmid- and the adenovirus-based siRNA-expressing vectors, i.e., psiSurv(A) and Adv-siSurv(A)—psiSurv(B) and Adv-siSurv(B), are the same.

By employing commonly used tumor cell lines, such as HeLa (cervical cancer), U251 (glioma), and MCF-7 (breast cancer) cells, we tested the effect of these siRNA-expressing adenoviral vectors on survivin expression. Seventy-two hours after infection with these survivin-oriented siRNA-expressing adenoviral vectors and relevant controls, we determined the expression levels of survivin by both RT-PCR and immunoblot analysis. We detected a decrease in survivin mRNA levels after transfection with either Adv-siSurv(A) or Adv-siSurv(B) in all three cell lines, whereas infection with Adv-siGL3B, a control adenovirus encoding siRNA against firefly luciferase, had only a minimal effect on survivin mRNA expression (Fig. 3A). Similarly, we also confirmed inhibition of survivin protein expression after infection with either Adv-siSurv(A) or Adv-siSurv(B) (Fig. 3B). Densitometric analysis revealed that the amount of survivin protein remaining in cells infected with Adv-siSurv(A) and Adv-siSurv(B) was 50 and 69% for HeLa, 73 and 23% for U251, and 61 and 69% for MCF-7, respectively, of that observed in cells infected with Adv-Null, which is devoid of an siRNA expression cassette. Again, Adv-siGL3B infection had little impact on the expression level of survivin protein in all the cell lines tested (Fig. 3B). Immunoblot analysis of cell lysates extracted 5 days after infection with these adenoviruses revealed that the gene knockdown effects with respect to survivin expression were sustained over this period (Fig. 3C). Densitometric analysis revealed that the amount of survivin protein remaining in cells infected with Adv-siSurv(A) and Adv-siSurv(B) was 89 and 40% for HeLa, 25 and 2% for U251, and 40 and 38% for MCF-7, respectively, of that observed in cells infected with Adv-Null, which is devoid of an siRNA expression cassette. These results indicate that adenovirus-mediated transduction of siRNA into these cancer cell lines was feasible. Since Adv-siSurv(B) appeared to exert a more efficient knockdown potential with respect to survivin expression compared to Adv-siSurv(A), we decided to choose Adv-siSurv(B) in subsequent experiments to test the antitumor efficacy of this type of adenovirus vector.

Adenoviral Transduction of siRNA against Survivin Elicited Apoptosis in Cancer Cells

We next examined the apoptosis-inducing potential of Adv-siSurv(B) in HeLa, U251, and MCF-7 cells via flow cytometric analysis of propidium iodide-stained cells. In all cell lines tested, infection with Adv-siSurv(B) increased the percentage of cells in the sub-G_0/G_1 fraction, whereas infection with Adv-siGL3B yielded only a marginal change in the pattern of DNA content (Fig. 4A). Cells within the sub-G_0/G_1 population represent apoptotic cells. The mean percentages ± standard deviations (SD) of apoptotic cells from three independent determinations are shown in Fig. 4B. The percentages of apoptotic cells after infection with Adv-siSurv(B), 17.6 ± 1.5 (HeLa), 14.0 ± 1.4 (U251), and 36.9 ± 5.3% (MCF-7), were much higher than those observed after infection with either Adv-Null, 2.7 ± 0.1 (HeLa), 4.7 ± 0.5 (U251), and 4.4 ± 0.5% (MCF-7), or Adv-siGL3B, 6.7 ± 0.8 (HeLa), 5.3 ± 0.6 (U251), and 5.1 ± 0.9% (MCF-7) ($n = 3$, $P < 0.01$, for all tested cell lines). To confirm that apoptosis induced by Adv-siSurv(B) infection was mediated by activation of caspases, we carried out immunoblot analysis for caspase-3, an executioner caspase. The polyclonal antibody used in this blot detects both procaspase-3 (32 kDa) and cleaved fragments of caspase-3 (p17–20), which are generated upon activation of caspase-3. In both HeLa and U251 cells, the amount of procaspase-3 protein decreased, along with a corresponding increase in the presence of

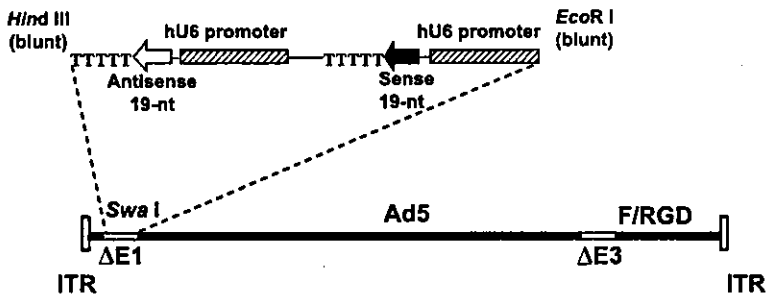

FIG. 2. A schematic presentation of the structure of the adenoviral vectors encoding U6 promoter-driven siRNA. The backbone of the adenoviral vectors used in this study was an E1- and E3-deleted serotype 5 adenovirus with a modified fiber F/RGD, harboring an integrin-binding RGD motif within the HI loop of its knob protein. The construction of this siRNA expression unit is of a tandem type, in which sense and antisense strands composing the siRNA duplex are independently transcribed by two human U6 promoters.

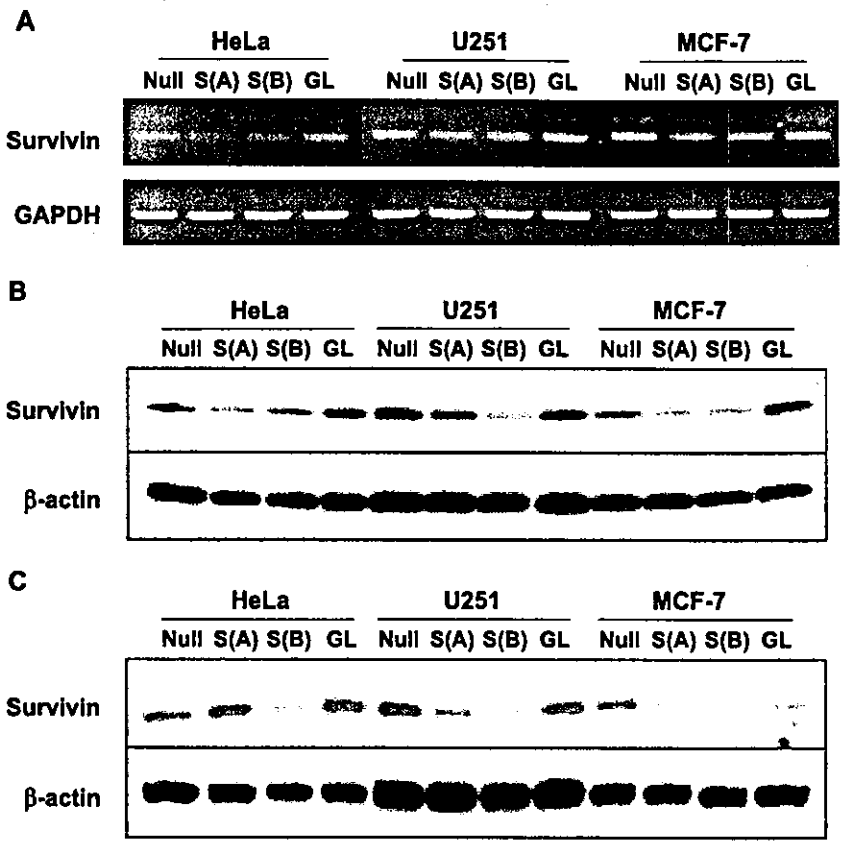

FIG. 3. The effect of adenoviral vectors encoding U6 promoter-driven siRNA against survivin on survivin expression in HeLa, U251, and MCF-7 cells. Adenoviral infection was performed at 3000 pt/cell. (A) RT-PCR analysis of survivin or GAPDH (internal control) mRNA expression performed 72 h after infection. (B) Immunoblot analysis of survivin or β-actin (internal control) protein expression performed 72 h after transfection. (C) Immunoblot analysis for survivin or β-actin (internal control) was performed 5 days after infection. Null, Adv-Null-infected cells; S(A), Adv-siSurv(A)-infected cells; S(B), Adv-siSurv(B)-infected cells; GL, Adv-siGL3B-infected cells. Adv-Null or Adv-siGL3B are control vectors encoding either no expression unit or siRNA against firefly luciferase. Adv-siSurv(A) and Adv-siSurv(B) are the adenoviral vectors that express siRNA against different sites of the survivin transcript.

cleaved fragments of caspase-3, following infection with Adv-siSurv(B) (Fig. 4C). Infection with Adv-siGL3B did not affect the status of caspase-3 (Fig. 4C). Taken together, adenovirus-mediated transfer of siRNA against survivin induced apoptosis in cancer cells.

Tumor Cells Infected with Adenovirus Expressing siRNA against Survivin Displayed Remarkably Attenuated Growth Potential *in Vitro*

We investigated whether the apoptosis-inducing potential of Adv-siSurv(B) mentioned above might result in suppression of tumor cell growth *in vitro*, as assessed by colony formation. We seeded cells infected with either Adv-siSurv(B) or control vector at 10^2 or 10^3 cells/six-well plate and cultured them for 12 days. Following staining of the resultant colonies with methylene blue, it was revealed that following infection with Adv-siSurv(B), all cancer cell lines tested exhibited markedly reduced proliferation capacity *in vitro*, whereas infection with adenovirus encoding siRNA against firefly luciferase yielded a minimal change in terms of cell growth (Fig. 5A). For quantification, we solubilized the stained colonies (formed after seeding 10^3 transfected cells) using HCl and performed colorimetric analysis using the resultant solution. The mean values ± SD from three determinations at A_{655} are shown in Fig. 5B. Values obtained from the Adv-siSurv(B)-infected cells, 0.044 ± 0.004 (HeLa), 0.014 ± 0.001 (U251), and 0.073 ± 0.010 (MCF-7), were much lower than those obtained from the Adv-Null-infected cells, 0.900 ± 0.030 (HeLa), 0.233 ± 0.016 (U251), and 1.043 ± 0.073 (MCF-7), or the Adv-siGL3B-infected cells, 0.846 ± 0.055 (HeLa), 0.185 ± 0.005 (U251), and 0.977 ± 0.012 (MCF-7) ($n = 3$, $P < 0.01$, for all the tested cell lines).

HeLa Cells Infected with Adenovirus Expressing siRNA against Survivin Nearly Lost Their Tumorigenicity *in Vivo*

We investigated the change in tumorigenicity *in vivo* of cells following Adv-siSurv(B) infection. We inoculated HeLa cells (5×10^6 cells) infected with either Adv-siSurv(B) or control vectors subcutaneously into nude mice and monitored the resultant tumor volume. All the mice in the Adv-Null group displayed exponentially growing tumors, with all the tumors reaching a size beyond 2000 mm^3 or developing an ulcer within 5 weeks (Fig. 6). All the mice in the Adv-siGL3B group also developed large tumors beyond 2000 mm^3 within 7 weeks after inoculation (Fig. 6). In contrast, all the mice in the Adv-siSurv(B) group developed significantly smaller tumors (Fig. 6). On day 18, the last assessable time point for the Adv-Null-treated group, the mice in

doi:10.1016/j.ymthe.2004.05.006

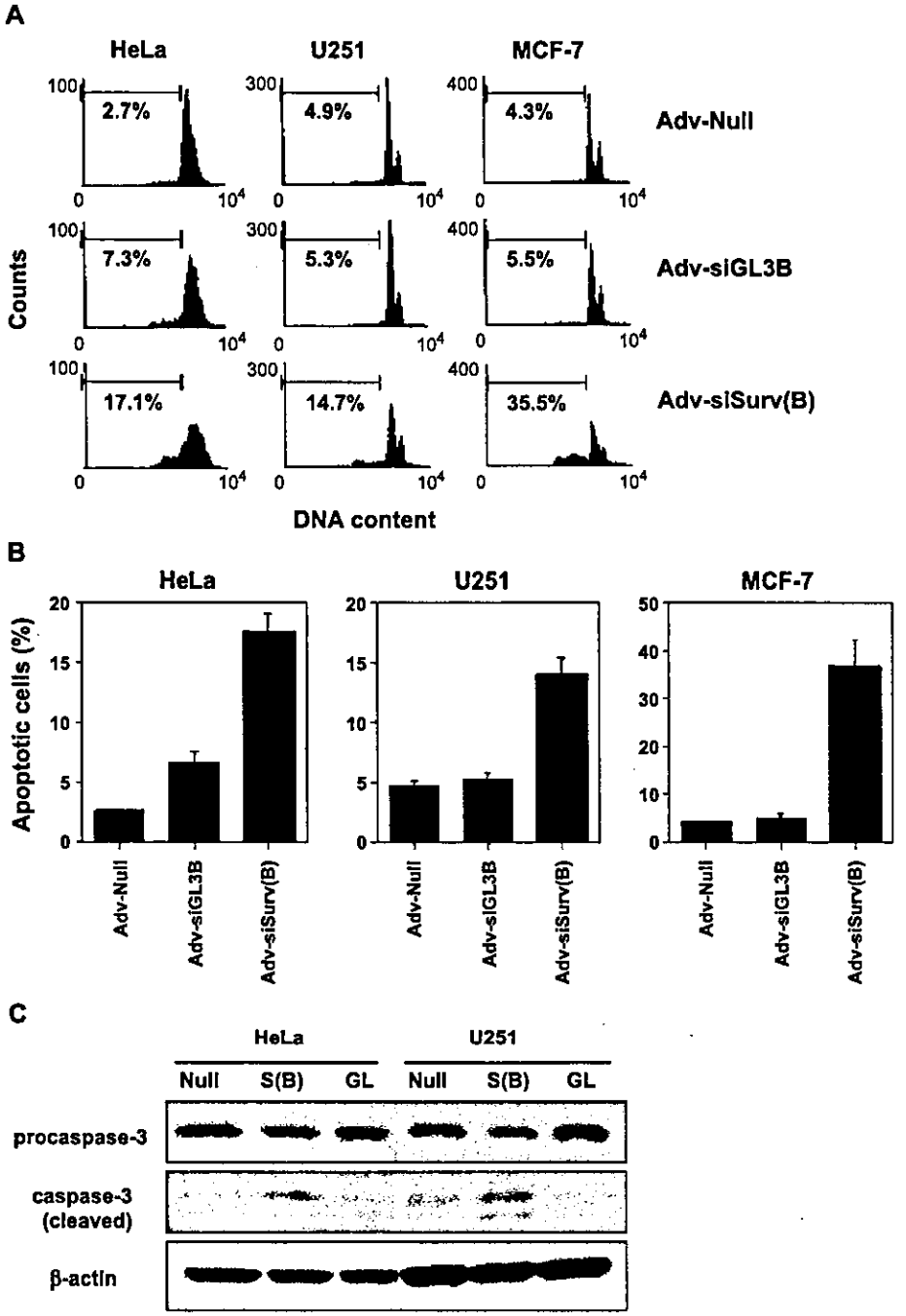

FIG. 4. Apoptosis-inducing potential of adenoviral vector encoding siRNA against survivin on HeLa, U251, and MCF-7 cells. Adenoviral infection was performed at 3000 pt/cell. (A) Flow-cytometric analysis of propidium iodide-stained cells was performed 6 days after infection. The percentages of hypodiploid cells are shown. The experiments were performed in triplicate and representative data are shown. (B) The mean percentages ± SD of hypodiploid cells from three determinations are shown. The experiments were repeated twice and similar results were obtained. Representative data are shown. (C) Immunoblot analysis for caspase-3 in HeLa and U251 cells performed 5 days after infection. The polyclonal antibody used detects both procaspase-3 (32 kDa) and cleaved fragments of caspase-3 (p17–20), which are generated upon activation of caspase-3.

the Adv-siSurv(B) group had a significantly smaller tumor size (mean ± SD) of 27 ± 10 mm^3, compared with a tumor size of 1012 ± 360 mm^3 for the Adv-Null group (n = 6, $P < 0.05$, Student t test) or a tumor size of 348 ± 295 mm^3 for the Adv-siGL3B group (n = 6, $P < 0.05$, Student t test). At this time point, the mice in the Adv-siGL3B group had a significantly smaller tumor size compared with that observed in the Adv-Null group (n = 6, $P < 0.05$, Student t test).

Intratumoral Injection of Adenovirus Encoding siRNA against Survivin Suppressed Tumor Growth in a Xenograft Model Using U251 Cells

Finally, we investigated the antitumor potential of Adv-siSurv(B) in a mouse xenograft model. We inoculated 5 × 10^6 U251 cells subcutaneously into nude mice. When the tumor size reached about 5 to 7 mm in diameter, six mice in each group received the first intratumoral injection of Adv-Null, Adv-siGL3B, or Adv-siSurv(B), each at 10^{10}

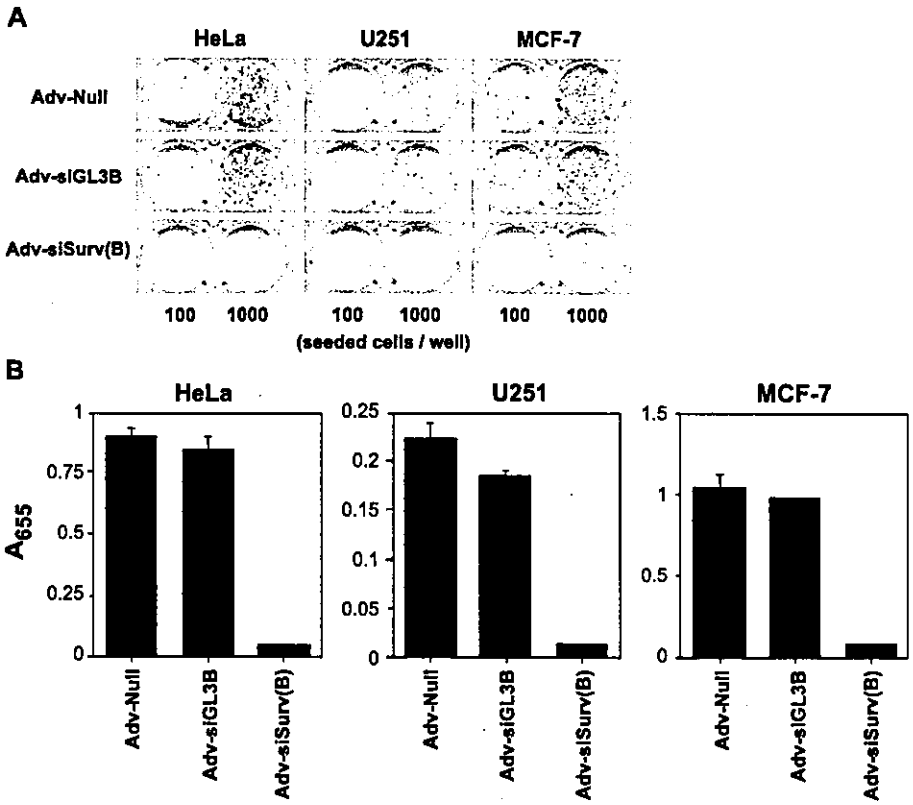

FIG. 5. The impact of adenoviral vectors encoding siRNA against survivin on growth of HeLa, U251, and MCF-7 cells *in vitro*. Adenoviral infection was performed at 3000 pt/cell. Twenty-four hours after infection, cells were seeded onto six-well culture plates at a concentration of 10^2 or 10^3 cells per well and were cultured for 12 days. (A) Photographs of the colonies stained by methylene blue. The experiments were performed in triplicate and representative data are shown. (B) The means ± SD of the A_{655}, as determined by colorimetric analysis, for the colonies from three determinations are shown. The experiments were repeated twice and similar results were obtained. Representative data are shown.

particles (pt) per tumor. We recorded the growth of the tumors from the first adenoviral injection (day 0). We repeated intratumoral injections of the same adenoviral vectors (10^{10} pt/tumor) at days 1, 2, 20, 21, 22, 41, 42, and 43, as shown in Fig. 7. As a result, all the mice in the Adv-Null group and the Adv-siGL3B group developed large tumors; three mice in the Adv-Null group and one mouse in the Adv-siGL3B group developed tumors beyond 2000 mm^3 on day 48. In contrast, the mice in the Adv-siSurv(B) group developed much smaller tumors (Fig. 7). On days 24, 26, 34, 38, 41, 45, and 48, the mice in the Adv-siSurv(B) group had a significantly smaller tumor size compared with that observed in the Adv-Null group ($n = 6$, $P < 0.05$, Student t test) or that observed in the Adv-siGL3B group ($n = 6$, $P < 0.05$, Student t test). On day 48, the last assessable time point for the Adv-Null and the Adv-siGL3B group, the mice in the Adv-siSurv(B) group had a significantly smaller tumor size (mean ± SD) of 431 ± 236 mm^3, compared with a tumor size of 1838 ± 415 mm^3 for the Adv-Null group ($n = 6$, $P < 0.05$, Student t test) or a tumor size of 1896 ± 204 mm^3 for the Adv-siGL3B group ($n = 6$, $P < 0.05$, Student t test). No significant difference in tumor size between the Adv-Null and the Adv-siGL3B groups was observed at any time point of this experiment.

Discussion

For the therapeutic application of siRNA technology, it may be critical to employ an efficient gene delivery system

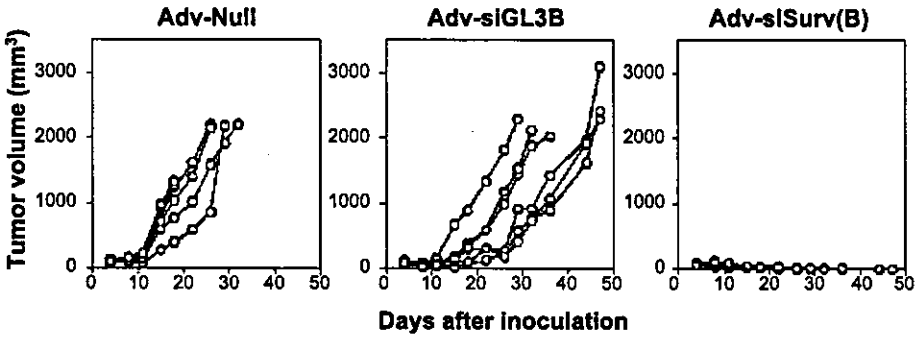

FIG. 6. The impact of adenoviral vectors encoding siRNA against survivin on tumorigenicity of HeLa cells *in vivo*. Adenoviral infection was performed at 3000 pt/cell. Twenty-four hours later, 5×10^6 infected cells were injected subcutaneously into a nude mouse. The tumor growth curves from individual animals are shown. Mice were humanely killed following development of a tumor larger than 2000 mm^3 or a tumor harboring an ulcer.

doi:10.1016/j.ymthe.2004.05.006

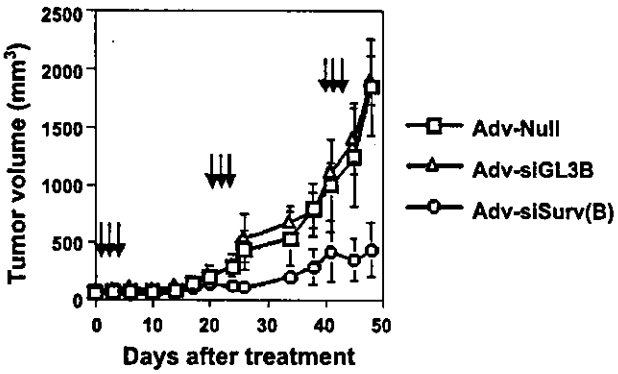

FIG. 7. The impact of adenoviral vectors encoding siRNA against survivin on growth of preestablished tumor in U251 xenograft model. Intratumoral injection of adenoviral vectors was begun when the tumor size reached about 5 to 7 mm in diameter. Each treatment (10^{10} pt/tumor) is shown as an arrow. The mean ± SD of the tumor volume for each group ($n = 6$) is shown for each time point. Mice were humanely killed following development of a tumor larger than 2000 mm^3.

for transduction of siRNA into target cells. The use of adenoviral vectors is considered to be a powerful tool in cancer gene therapy because they have been shown to transduce genes efficiently into many types of cancer cells. The adenoviral vectors used in this study contain a modified fiber knob protein, genetically modified to contain an integrin-binding RGD motif in its HI loop so as to widen the host range of infection further (Fig. 2) [35]. The vector-based siRNA expression systems reported so far may be roughly divided into two types: tandem type and hairpin type [11–19]. In a tandem-type vector, the sense and antisense strands composing the siRNA duplex are independently transcribed by two promoters. On the other hand, in a hairpin-type vector, a single promoter drives siRNA expression as a fold-back stem–loop structure that produces siRNAs after intramolecular processing. In this study, we employed a U6-driven, tandem-type siRNA expression construct for application to adenoviral systems (Fig. 2) and succeeded in mediating suppression of target gene (i.e., survivin) expression (Figs. 3A, 3B, and 3C). In contrast to the tandem-type system, the hairpin-type siRNA expression system requires cellular Dicer activity for processing of dsRNAs with a loop motif in the generation of functioning siRNAs [19]. It is possible that Dicer activities are diverse among different cancer cell types. Therefore, the superiority between tandem- and hairpin-type siRNA expression systems might depend on cell type. Currently, we are comparing the efficacy of adenoviral vector-based siRNA expression in various cancer cell lines under these two types of systems.

Since *survivin* represents one of the most tumor-specific genes in the human genome, its protein has been considered to be a promising molecular target for cancer therapy [36]. The molecular mechanism underlying the antiapoptotic function of survivin remains unclear. It has been demonstrated that survivin is able to bind to caspase-3 and caspase-7 *in vitro*. Moreover, it is proposed that survivin may inhibit apoptosis through suppression of caspase activities [27]. However, comparison of the X-ray crystallographic structure of survivin with that of the XIAP (BIR2):caspase-3 complex fails to suggest how survivin might suppress caspase-3 directly [37]. Although the single BIR domain in the survivin protein has been shown to be closely related to the XIAP BIR3 domain on the basis of three-dimensional structure, a manifest evidence of direct binding between survivin and caspase-9 remains to be shown [38]. Recently, Reed and colleagues demonstrated that survivin formed complexes with hepatitis B X-interacting protein (HBXIP) and that survivin–HBXIP complexes could bind to procaspase-9, thus preventing its recruitment to apoptotic protease-activating factor-1 [39]. Wu and colleagues have reported that survivin can bind to the proapoptotic mitochondrial protein Smac/DIABLO, both *in vitro* and *in vivo*. Furthermore, they proposed that binding of survivin to Smac/DIABLO may reduce Smac/DIABLO antagonism to IAPs, such as XIAP, therefore enabling free XIAP to block caspases directly [40]. In this study, we demonstrated that adenovirus encoding siRNA against survivin, by itself, elicited apoptosis in cancer cells (Figs. 4A, 4B, and 4C). These results are consistent with those of Altieri and colleagues, who report that functional ablation of survivin using a dominant-negative mutant, survivin (T34A), elicited apoptosis in cancer cells without the necessity for additional inducers of apoptosis [30]. It may be reasonable to hypothesize that cancer cells survive based on the predominance of anti-apoptotic over proapoptotic molecules and that the disturbance of such a balance by transducing siRNA against survivin or a dominant-negative mutant of this protein might lead to cancer cell apoptosis. However, the possibility cannot be ruled out that abolishment of survivin expression or its function may trigger some proapoptotic signal upstream of the mitochondria.

We demonstrated that adenovirally transduced siRNA against survivin exerted a powerful antitumor effect both *in vitro* (Figs. 5A and 5B) and *in vivo* (Figs. 6 and 7). In tumorigenicity experiments, cells infected with an adenovirus expressing control siRNA, namely Adv-siGL3B, displayed some delay with respect to tumor growth compared to cells infected with an adenovirus devoid of an expression cassette, i.e., Adv-Null (Fig. 6). The underlying mechanism for this observation is not clear. One possibility is that this observation represents an off-target gene regulation effect by the siRNA against firefly luciferase, a gene that does not exist in human cells. Many reports have alluded to the prominent specificity displayed by siRNAs, suggesting a requirement for nearly perfect identity of the target site sequences and corresponding siRNA [41–43]. However, in recent studies, the possibilities of off-target effects of siRNA have

been revealed by gene expression profiling studies [44,45]. Interestingly, one of these reports has shown that, using a high concentration of siRNA for transfection, siRNAs against different target molecules cause a nonspecific induction (not knockdown) of a large number of common genes, including some apoptosis-related genes, for example, *BAK, bcl-2,* and *death-associating protein kinase* (*DAPK*), or stress-response genes [44]. It is possible that nonspecific induction of such molecules may contribute to the delay in tumor formation observed following inoculation of cells infected with Adv-siGL3B. Further studies might be needed to both determine and refine the specificity of siRNA transduced by expression vectors, including adenoviral vectors.

In the present study, we developed recombinant adenoviral vectors encoding siRNA against the survivin transcript and explored the impact of these novel vectors on three representative cancer cell lines. In all cell lines examined, a knockdown of survivin expression was confirmed following infection with these adenoviruses, which resulted in apoptotic cell death. Cells infected with these vectors nearly lost their tumorigenicity following inoculation into nude mice. Intratumoral injection with these vectors significantly suppressed tumor growth in a mouse xenograft model. This novel strategy may be a promising tool for cancer gene therapy.

Materials and Methods

Cell culture. The human embryonic kidney 293T cells were obtained from GenHunter (Nashville, TN, USA) and were maintained in Dulbecco's modified Eagle's medium containing 10% fetal bovine serum, 0.2% sodium bicarbonate, 2 mM glutamine, at 37°C in a humidified atmosphere of 5% carbon dioxide and 95% air. The human cancer cell lines, HeLa, U251, and MCF-7, were obtained from the American Type Culture Collection (Manassas, VA, USA) and were maintained under conditions recommended by this organization.

Plasmid vectors. Tandem-type siRNA expression vectors in this study were constructed as described previously [12]. In brief, a human U6 promoter-driven expression cassette for the antisense strand was amplified by PCR and inserted into a plasmid vector containing another U6 promoter-driven expression cassette for the sense strand, resulting in a plasmid vector harboring two separate U6 promoter-driven expression units for each RNA strand of siRNA. Sequences inserted immediately downstream of the U6 promoter were as follows (only sense sequence shown): psiGL3B [12] against firefly luciferase, 5′-GTGCGCTGCTGGTGCCAAC-3′; psiSurv(A) against survivin, 5′-GAGCCAAGAACAAAATTGC-3′; psiSurv(B) against survivin, 5′-GAAAGTGCGCCGTGCCATC-3′. pUC19, a control vector without a U6 promoter-driven expression cassette, was obtained from New England Biolabs (Beverly, MA, USA). Transfection of plasmid DNA was carried out by lipofection using Lipofectamine2000 (Invitrogen, Carlsbad, CA, USA) as described by the manufacturer.

Adenoviral vectors. All the recombinant adenoviral vectors used in this study were based on the E1- and E3-deleted serotype 5 adenovirus with a modified fiber F/RGD, harboring an integrin-binding RGD-motif within the HI loop of its knob protein [35]. In the first step, a 14,896-bp *Eco*RI fragment (including the right side of the adenoviral genome) of pWEAxKM-F/RGD [35] was joined with a 24,505-bp *Eco*RI fragment (including the left side of the adenoviral genome) of pL_{RI} [46], generating the cosmid vector pWEAx-F/RGD. Then, a 592-bp *Eco*RI–*Hin*dIII fragment, which included the tandemly arranged U6 promoter-driven siRNA expression cassette of psiGL3B, psiSurv(A), or psiSurv(B), was blunt-ended and inserted into the *Swa*I site of pWEAx-F/RGD according to the direction shown in Fig. 2, resulting in the cosmid vectors pWEAxsiGL3B-F/RGD, pWEAxsiSurv(A)-F/RGD, and pWEAxsiSurv(B)-F/RGD, respectively. For the generation of recombinant adenovirus, each cosmid was transfected into 293 cells by lipofection using Lipofectamine2000 reagent (Invitrogen). Plaques arising from the transfected 293 cells were isolated and evaluated by restriction enzyme digestion of the viral genome and sequencing of the expression units. The resultant adenoviral vectors, Ax-F/RGD (Adv-Null), a control adenovirus devoid of an expression cassette, and AxsiGL3B-F/RGD (Adv-siGL3B), AxsiSurv(A)-F/RGD (Adv-siSurv(A)), and AxsiSurv(B)-F/RGD (Adv-siSurv(B)), all carrying expression cassettes for siRNA against corresponding target transcripts, were expanded in 293 cells and purified by cesium chloride ultracentrifugation [47]. Purified viruses were dialyzed in phosphate-buffered saline (PBS) with 10% glycerol and stored at −70°C until use. To determine the viral concentration (pt/ml), the viral solution was incubated in 0.1% sodium dodecyl sulfate (SDS) and A_{260} measured [48]. The concentration was defined as pt/ml = $A_{260} \times (1.1 \times 10^{12})$. Before use, contamination with replication-competent viruses in the viral stock was ruled out by PCR analysis using primers specific for E1A, forward primer 5′-ATTACCGAAGAAATGGCCGC-3′, reverse primer 5′-CCCATTTAACACGCCATGCA-3′; E1B, forward primer 5′-CGGCTGCTGTTGCTTTTTTG-3′, reverse primer 5′-GTATCTTCATCGCTAGAGCC-3′; and E2B (positive control), forward primer 5′-TCGTTTCTCAGCAGCTGTTG-3′, reverse primer 5′-CATCTGAACTCAAAGCGTGG-3′ [49]. Adenoviral infection was performed essentially as described previously [50]. All infection experiments were performed at 3000 pt/cell, a condition that enabled almost 100% transduction of transgenes into the cancer cells used in this study (data not shown). In a preliminary experiment, the transduction efficiency at 100 pt/cell was 96% for HeLa cells, 79% for U251 cells, and 56% for MCF-7 cells, determined using an EGFP-expressing adenoviral vector with F/RGD (data not shown).

RT-PCR analysis. Total RNA from transfected cells was isolated using the RNeasy Kit (Qiagen, Valencia, CA, USA) according to the manufacturer's instructions. Reverse transcription was performed at 42°C for 60 min using oligo$(dT)_{12-18}$ (Amersham, Little Chalfont, UK). The primers for PCR amplification used in this study were as follows: survivin, forward primer 5′-ACGAGCCAGACTTGGCCCAGTGTT-3′, reverse primer 5′-TCAATCCATGGCAGCCAGCTGCTC-3′; GAPDH (internal control), forward primer 5′-CCACCCATGGCAAATTCCATGGCA-3′, reverse primer 5′-TCTAGACGGCAGGTCAGGTCCACC-3′. The PCR conditions were 96°C for 0.5 min, 65°C for 0.5 min, and 72°C for 1 min, over 24 cycles. PCR products were visualized with ethidium bromide on 2% agarose gels.

Immunoblot analysis. Total cell lysates from transfected cells were extracted with lysis buffer containing 10 mM Tris–HCl (pH 8.0), 0.2% NP-40, 1 mM EDTA, and 2% SDS. Immunoblot analysis was then carried out essentially as described previously [50]. The primary antibody was mouse anti-survivin monoclonal antibody (2802; Cell Signaling Technology, Beverly, MA, USA), rabbit anti-XIAP polyclonal antibody (X-2503; Sigma, St. Louis, MO, USA), rabbit anti-caspase-3 polyclonal antibody (9662; Cell Signaling Technology), or mouse anti-β-actin monoclonal antibody (A-5441; Sigma). The secondary antibody was either horseradish peroxidase-conjugated rabbit anti-mouse IgG+A+M (H+L) (Zymed Laboratories, San Francisco, CA, USA), in the case of samples treated with primary antibodies to survivin or β-actin, or donkey anti-rabbit IgG, peroxidase-linked species-specific $F(ab')_2$ fragment (Amersham), in the case of samples treated with primary antibodies to caspase-3 or XIAP. Chemiluminescence detection was carried out using the ECL Kit (Amersham) according to the manufacturer's instructions.

Cell cycle analysis. Cell cycle analysis was performed on cells following propidium iodide incorporation as described previously [50]. Briefly, cells were removed by trypsinization 6 days after adenoviral infection, washed

in PBS, and fixed with 70% ethanol. Fixed samples were centrifuged, treated with RNase (0.25 mg/ml), and resuspended in propidium iodide (50 μg/ml). Propidium iodide-stained cells were analyzed by a FACS Calibur (Becton–Dickinson, San Jose, CA, USA) flow cytometer.

Colony forming assay. Twenty-four hours after adenoviral infection, cells were seeded onto six-well culture plates at a concentration of 10^2 or 10^3 cells per well and were cultured for 12 days. Following removal of the medium, the wells were rinsed twice with PBS. Glutaraldehyde (1.25%) in PBS was added to each well and the plates were incubated for 30 min at room temperature to allow for cell fixation. After two rinses with distilled water, 0.05% methylene blue solution was added to each well and plates were incubated for 30 min at room temperature to facilitate staining of the colonies. After two rinses with distilled water, the plates were dried and photographed. For quantification of cell growth, stained colonies were solubilized by adding 1 ml of 0.33 N HCl solution per well. Following sampling of 100 μl of the resultant solution, the A_{655} was determined.

Animal experiments. All mice ware fed *ad libitum* and received human care in compliance with the institution's guidelines for the care and use of laboratory animals in research. Five-week-old female BALB/cAnNCjr-nu/nu mice were purchased from Japan Charles River (Yokohama, Japan). In tumorigenicity experiments, HeLa cells were infected with Adv-Null, Adv-siGL3B, or Adv-siSurv(B) at 3000 pt/cell. Twenty-four hours later, 5×10^6 infected cells were suspended in 50 μl of PBS and injected subcutaneously into the right flank of each mouse. The tumor diameter was measured, and the volume (product of 0.4 × largest diameter × smallest diameter × smallest diameter) was calculated. Mice were humanely killed following development of a tumor larger than 2000 mm^3 or a tumor harboring an ulcer. In *in vivo* treatment experiments, 5×10^6 U251 cells were suspended in 100 μl of PBS and injected subcutaneously into the right flank of each mouse. When the tumor size reached about 5 to 7 mm in diameter, six mice in each group received the first intratumoral injection of Adv-Null, Adv-siGL3B, or Adv-siSurv(B), each at 10^{10} pt/tumor. The volume of tumors was recorded as mentioned above from the first injection (day 0). Intratumoral injections of the adenoviral vectors at the same dose were repeated as indicated in Fig. 7.

Statistical analysis. Statistical comparison of the data was performed using a Student *t* test. A *P* value of less than 0.05 was considered to be significant.

Acknowledgments

We thank Aiko Kuroishi, Hanae Inoue, and Yuko Tani for technical assistance. This work was supported in part by a Grant-in-Aid for JSPS Fellows to H.U. and grants to H.H. from the Ministry of Education, Science, and Culture of Japan and from the Terumo Foundation, Kanagawa, Japan.

RECEIVED FOR PUBLICATION SEPTEMBER 9, 2003; ACCEPTED MAY 4, 2004.

References

1. Fire, A., *et al.* (1998). Potent and specific genetic interference by double-stranded RNA in Caenorhabditis elegans. *Nature* **391:** 806–811.
2. Sharp, P. A. (2001). RNA interference—2001. *Genes Dev.* **15:** 485–490.
3. Hutvagner, G., and Zamore, P. D. (2002). RNAi: nature abhors a double-strand. *Curr. Opin. Genet. Dev.* **12:** 225–232.
4. Hannon, G. J. (2002). RNA interference. *Nature* **418:** 244–251.
5. Bernstein, E., Caudy, A. A., Hammond, S. M., and Hannon, G. J. (2001). Role for a bidentate ribonuclease in the initiation step of RNA interference. *Nature* **409:** 363–366.
6. Hammond, S. M., Bernstein, E., Beach, D., and Hannon, G. J. (2000). An RNA-directed nuclease mediates post-transcriptional gene silencing in Drosophila cells. *Nature* **404:** 293–296.
7. Hammond, S. M., Boettcher, S., Caudy, A. A., Kobayashi, R., and Hannon, G. J. (2001). Argonaute2, a link between genetic and biochemical analyses of RNAi. *Science* **293:** 1146–1150.
8. Elbashir, S. M., *et al.* (2001). Duplexes of 21-nucleotide RNAs mediate RNA interference in cultured mammalian cells. *Nature* **411:** 494–498.
9. Manche, L., Green, S. R., Schmedt, C., and Mathews, M. B. (1992). Interactions between double-stranded RNA regulators and the protein kinase DAI. *Mol. Cell. Biol.* **12:** 5238–5248.
10. Minks, M. A., West, D. K., Benvin, S., and Baglioni, C. (1979). Structural requirements of double-stranded RNA for the activation of 2′,5′-oligo(A) polymerase and protein kinase of interferon-treated HeLa cells. *J. Biol. Chem.* **254:** 10180–10183.
11. Brummelkamp, T. R., Bernards, R., and Agami, R. (2002). A system for stable expression of short interfering RNAs in mammalian cells. *Science* **296:** 550–553.
12. Miyagishi, M., and Taira, K. (2002). U6 promoter-driven siRNAs with four uridine 3′ overhangs efficiently suppress targeted gene expression in mammalian cells *Nat. Biotechnol.* **20:** 497–500.
13. Lee, N. S., *et al.* (2002). Expression of small interfering RNAs targeted against HIV-1 rev transcripts in human cells. *Nat. Biotechnol.* **20:** 500–505.
14. Paul, C. P., Good, P. D., Winer, I., and Engelke, D. R. (2002). Effective expression of small interfering RNA in human cells. *Nat. Biotechnol.* **20:** 505–508.
15. Paddison, P. J., Caudy, A. A., Bernstein, E., Hannon, G. J., and Conklin, D. S. (2002). Short hairpin RNAs (shRNAs) induce sequence-specific silencing in mammalian cells. *Genes Dev.* **16:** 948–958.
16. Sui, G., *et al.* (2002). A DNA vector-based RNAi technology to suppress gene expression in mammalian cells. *Proc. Natl. Acad. Sci. USA* **99:** 5515–5520.
17. Yu, J. Y., DeRuiter, S. L., and Turner, D. L. (2002). RNA interference by expression of short-interfering RNAs and hairpin RNAs in mammalian cells. *Proc. Natl. Acad. Sci. USA* **99:** 6047–6052.
18. McManus, M. T., Petersen, C. P., Haines, B. B., Chen, J., and Sharp, P. A. (2002). Gene silencing using micro-RNA designed hairpins. *RNA* **8:** 842–850.
19. Kawasaki, H., and Taira, K. (2003). Short hairpin type of dsRNAs that are controlled by tRNA(Val) promoter significantly induce RNAi-mediated gene silencing in the cytoplasm of human cells. *Nucleic Acids Res.* **31:** 700–707.
20. Crook, N. E., Clem, R. J., and Miller, L. K. (1993). An apoptosis-inhibiting baculovirus gene with a zinc finger-like motif. *J. Virol.* **67:** 2168–2174.
21. Liston, P., *et al.* (1996). Suppresion of apoptosis in mammalian cells by NAIP and a related family of IAP genes. *Nature* **379:** 349–353.
22. Deveraux, Q. L., Takahashi, R., Salvesen, G. S., and Reed, J. C. (1997). X-linked IAP is a direct inhibitor of cell-death proteases. *Nature* **388:** 300–304.
23. Takahashi, R., *et al.* (1998). A single BIR domain of XIAP sufficient for inhibiting caspases. *J. Biol. Chem.* **273:** 7787–7790.
24. Ambrosini, G., Adida, C., and Altieri, D. C. (1997). A novel anti-apoptosis gene, survivin, expressed in cancer and lymphoma. *Nat. Med.* **3:** 917–921.
25. Reed, J. C., and Bischoff, J. R. (2000). BIRinging chromosomes through cell division—and survivin' the experience. *Cell* **102:** 545–548.
26. Li, F., *et al.* (1998). Control of apoptosis and mitotic spindle checkpoint by survivin. *Nature* **396:** 580–584.
27. Tamm, I., *et al.* (1998). IAP-family protein survivin inhibits caspase activity and apoptosis induced by Fas (CD95), Bax, caspases, and anticancer drugs. *Cancer Res.* **58:** 5315–5320.
28. Kobayashi, K., Hatano, M., Otaki, M., Ogasawara, T., and Tokuhisa, T. (1999). Expression of a murine homologue of the inhibitor of apoptosis protein is related to cell proliferation. *Proc. Natl. Acad. Sci. USA* **96:** 1457–1462.
29. Lu, C. D., Altieri, D. C., and Tanigawa, N. (1998). Expression of a novel antiapoptosis gene, survivin, correlated with tumor cell apoptosis and p53 accumulation in gastric carcinomas. *Cancer Res.* **58:** 1808–1812.
30. Mesri, M., Wall, N. R., Li, J., Kim, R. W., and Altieri, D. C. (2001). Cancer gene therapy using a survivin mutant adenovirus. *J. Clin. Invest.* **108:** 981–990.
31. Ambrosini, G., Adida, C., Sirugo, G., and Altieri, D. C. (1998). Induction of apoptosis and inhibition of cell proliferation by survivin gene targeting. *J. Biol. Chem.* **273:** 11177–11182.
32. Olie, R. A., *et al.* (2000). A novel antisense oligonucleotide targeting survivin expression induces apoptosis and sensitizes lung cancer cells to chemotherapy. *Cancer Res.* **60:** 2805–2809.
33. Pennati, M., *et al.* (2002). Ribozyme-mediated attenuation of survivin expression sensitizes human melanoma cells to cisplatin-induced apoptosis. *J. Clin. Invest.* **109:** 285–286.
34. Choi, K. S., Lee, T. H., and Jung, M. H. (2003). Ribozyme-mediated cleavage of the human survivin mRNA and inhibition of antiapoptotic function of survivin in MCF-7 cells. *Cancer Gene Ther.* **10:** 87–95.
35. Nakamura, T., Sato, K., and Hamada, H. (2002). Effective gene transfer to human melanomas via integrin-targeted adenoviral vectors. *Hum. Gene Ther.* **13:** 613–626.
36. Velculescu, V. E., *et al.* (1999). Analysis of human transcriptomes. *Nat. Genet.* **23:** 387–388.
37. Riedl, S. J., *et al.* (2001). Structural basis for the inhibition of caspase-3 by XIAP. *Cell* **104:** 791–800.
38. Shi, Y. (2000). Survivin structure: crystal unclear. *Nat. Struct. Biol.* **7:** 620–623.
39. Marusawa, H., *et al.* (2003). HBXIP functions as a cofactor of survivin in apoptosis suppression. *EMBO J.* **22:** 2729–2740.
40. Song, Z., Yao, X., and Wu, M. (2003). Direct interaction between survivin and Smac/